AD-A085 980 AUBURN UNIV ALA ENGINEERING EXPERIMENT STATION F/G 19/5
QUANTIZATION EFFECTS ON TARGET HANDOFF FROM TV TO IR DIGITIZED --ETC(U)
SEP 79 J S BOLAND, H S RANGANATH DAAK40-79-M-0104

UNCLASSIFIED NL

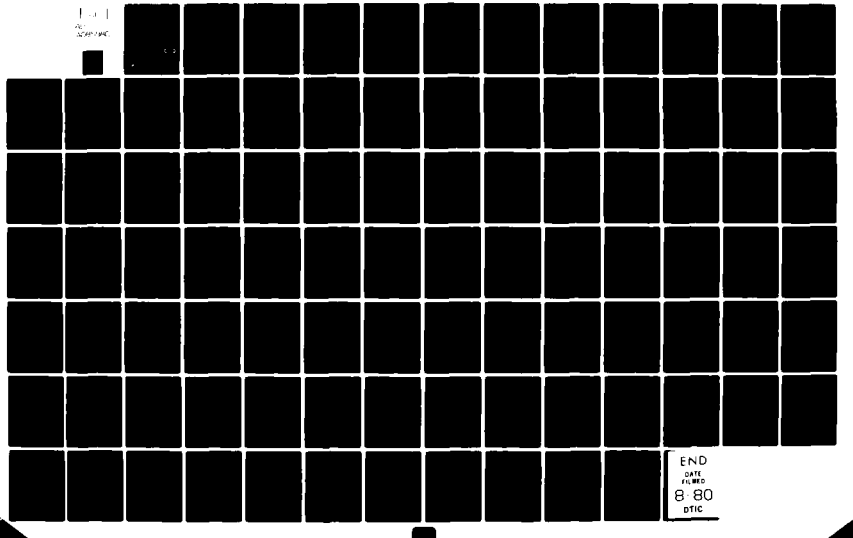

END
DATE FILMED
8-80
DTIC

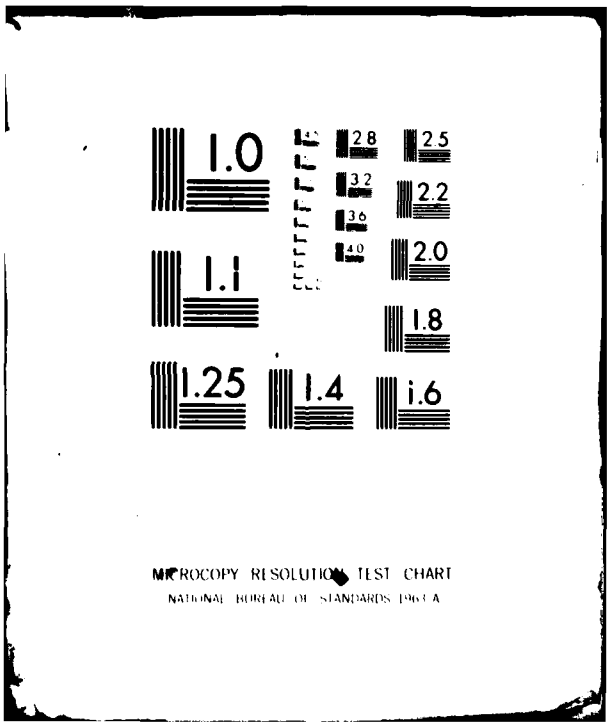
1.0
1.1
1.25
1.4
1.6
2.8
3.2
3.6
4.0
2.5
2.2
2.0
1.8
MICROCOPY RESOLUTION TEST CHART
NATIONAL BUREAU OF STANDARDS 1963-A

QUANTIZATION EFFECTS ON TARGET HANDOFF FROM TV TO IR DIGITIZED SCENES

BY

J. S. Boland, III and H. S. Ranganath

Electrical Engineering Department
Auburn University
Auburn, Alabama 36830

Final Technical Report
For the Period 21 March 1979 - 15 September 1979

This research work was supported by
US Army Missile Command
Redstone Arsenal, Alabama 35809
under Contract DAAK40-79-M-0104

ENGINEERING EXPERIMENT STATION
Auburn University
Auburn, Alabama 36830

15 September 1979

SECURITY CLASSIFICATION OF THIS PAGE (When Data Entered)

REPORT DOCUMENTATION PAGE

READ INSTRUCTIONS BEFORE COMPLETING FORM

1. REPORT NUMBER
2. GOVT ACCESSION NO. AD-A085 980
3. RECIPIENT'S CATALOG NUMBER

4. TITLE (and Subtitle)
Quantization Effects on Target Handoff from TV to IR Digitized Scenes.

5. TYPE OF REPORT & PERIOD COVERED
Final Technical Report. 21 Mar [redacted] – 15 Sep 79

6. PERFORMING ORG. REPORT NUMBER

7. AUTHOR(s)
J. S. Boland, III and H. S. Ranganath

8. CONTRACT OR GRANT NUMBER(s)
DAAK40-79-M-0104

9. PERFORMING ORGANIZATION NAME AND ADDRESS
Engineering Experiment Station
Auburn University
Auburn, AL 36830

10. PROGRAM ELEMENT, PROJECT, TASK AREA & WORK UNIT NUMBERS
12 92

11. CONTROLLING OFFICE NAME AND ADDRESS
Headquarters, US Army Missile Command
ATTN: DRSMI-IYB/Elenburg
Redstone Arsenal, AL 35809

12. REPORT DATE
15 Sep 79

13. NUMBER OF PAGES
90

14. MONITORING AGENCY NAME & ADDRESS (if different from Controlling Office)

15. SECURITY CLASS. (of this report)
UNCLASSIFIED

15a. DECLASSIFICATION/DOWNGRADING SCHEDULE

16. DISTRIBUTION STATEMENT (of this Report)

Cleared for Public Release; Distribution Unlimited

17. DISTRIBUTION STATEMENT (of the abstract entered in Block 20, if different from Report)

18. SUPPLEMENTARY NOTES

19. KEY WORDS (Continue on reverse side if necessary and identify by block number)
Correlation, Target Handoff, Image Correlation

Accession For
NTIS GRA&I
DDC TAB
Unannounced
Justification
By
Distribution/
Availability Codes
Dist | Special
A

20. ABSTRACT (Continue on reverse side if necessary and identify by block number)

This report presents the results and conclusions based on the analysis and simulation performed on day TV and IR digitized scenes. Specifically, the effects of four-bit quantization vs eight-bit quantization and of scale factor errors on correlation accuracy are given. A new more reliable correlation algorithm is also given.

DD FORM 1 JAN 73 1473 EDITION OF 1 NOV 65 IS OBSOLETE

UNCLASSIFIED

SECURITY CLASSIFICATION OF THIS PAGE (When Data Entered)

TABLE OF CONTENTS

Page

LIST OF FIGURES 3

LIST OF TABLES 5

I. INTRODUCTION 7

A. Scope of Work
B. Organization of Report

II. IMPROVED METHOD FOR TV-TO-TV CORRELATION 9

III. TV-TO-IR CORRELATION ALGORITHM 29

Equalization of Spatial Resolutions of HR and LR Videos
Edge Extraction
Sensitivity of Correlator to Field of View Errors
Effect of Threshold on Correlation Process
Automatic Threshold and Quantization

1. Choosing threshold by intuition
2. Area average method
3. Quantization based on mean and standard deviation of gradient images

TV-to-IR Correlation Simulation

Scene 1 - NASA tower
Scene 2 - Parking lot
Scene 3 - Water tank
Scene 4 - Rock quarry

Comparison of Four Methods

IV. EFFECT OF QUANTIZATION TO SIXTEEN LEVELS 53

Quantization by Truncation
Quantization based on dynamic range of pixel values
Histogram equalization

V. IMPROVED METHOD FOR TV-TO-IR CORRELATION. 68

TV-to-IR Correlation Simulation Using
Improved Method on 256 Level Video
TV-to-IR Correlation Simulation Using
Improved Method on 16 Level Video

VI. CONCLUSIONS AND RECOMMENDATIONS 89

LIST OF FIGURES

		Page
1.	Correlation values of first four peaks before and after improved analysis.	12
2.	Correlation values of first four peaks before and after improved analysis.	13
3.	Correlation values of first four peaks before and after improved analysis for jeep in front of the fence	23
4.	Correlation values of first four peaks before and after improved analysis for jeep behind the fence	24
5.	Correlation values of first four peaks before and after improved analysis for jeep in the parking lot.	25
6.	Correlation values of first four peaks before and after improved analysis for parking lot scene.	26
7.	Correlation values of first four peaks before and after improved analysis for NASA tower scene.	27
8.	Correlation values of first four peaks before and after improved analysis for water tank scene	28
9.	Layout for the estimation of gradient value associated with pixel (i,j).	31
10.	Weighting matrices for sobel edge detector.	31
11.	Layout for the quantization of GLRV (I,J)	39
12.	Pictorial representation of quantization process.	41
13.	Plot of correlation values of first four peaks before and after improved analysis	73

14. Correlation values of first four peaks before and after improved analysis. 77

15. Correlation values of first four peaks before and after improved analysis. 78

16. First four peaks before and after improved analysis for 16 level video (truncation) 79

17. First four peaks before and after improved method for 16 level video (truncation) 80

18. First four peaks before and after improved method for 16 level video (dynamic range slicing) 81

19. First four peaks before and after improved method for 16 level video (dynamic range slicing) 82

LIST OF TABLES

		Page
1.	Line average quantizer with 32 x 32 reference array.	16
2.	Analog line average quantizer with 32 x 32 reference array.	17
3.	Area average quantizer with 32 x 32 reference array.	18
4.	Line average quantizer with 16 x 16 reference array.	19
5.	Analog line average quantizer with 16 x 16 reference array.	20
6.	Area average quantizer with 16 x 16 reference array.	21
7.	Details of figures 3 through 8.	22
8.	NASA tower.	33
9.	Parking lot	34
10.	Effect of threshold on correlation process for parking lot scene.	36
11.	Correlation methods used in Tables 12 through 23.	48
12.	NASA tower TV-to-IR correlation	49
13.	Parking lot TV-to-IR correlation.	50
14.	Water tank TV-to-IR correlation	51
15.	Rock quarry TV-to-IR correlation.	52
16.	NASA tower, TV-to-IR correlation with quantization to 4 bits by truncation.	60

17. Parking lot, TV-to-IR correlation with quantization to 4 bits by truncation. 61

18. Water tower, TV-to-IR correlation with quantization to 4 bits by truncation. 62

19. Rock quarry, TV-to-IR correlation with quantization to 4 bits by truncation. 63

20. NASA tower, TV-to-IR correlation with quantization to four bits over dynamic range. 64

21. Parking lot, TV-to-IR correlation with quantization to four bits over dynamic range. 65

22. Water tower, TV-to-IR correlation with quantization to four bits over dynamic range. 66

23. Rock quarry, TV-to-IR correlation with quantization to four bits over dynamic range. 67

24. TV-to-IR correlation using the improved method 83

25. TV-to-IR correlation using the improved method 84

26. TV-to-IR correlation using the improved method for 16 level video obtained by truncation. 85

27. TV-to-IR correlation using the improved method for 16 level video obtained by truncation. 86

28. TV-to-IR correlation using the improved method for 16 level video obtained by slicing the dynamic range. 87

29. TV-to-IR correlation using the improved method for 16 level video obtained by slicing the dynamic range. 88

I. INTRODUCTION

Currently the US Army is developing a fire control system for the acquisition, identification, tracking and handoff of targets to an imaging missile seeker in a true fire and forget mode. A key technical issue in the above system is an algorithm and hardware which can accomplish automatic target handoff between a precision pointing and tracking system (PTS) and the missile seeker. The PTS can either be a high resolution day TV system or a forward looking infrared (FLIR) system. The missile, which is usually lower resolution because of size and costs constraints, can be a day TV or an infrared imaging seeker (IRIS) system. Therefore target handoff must be accomplished between two similar sensors (e.g., between the PTS high resolution day TV and the missile low resolution day TV system) or between two dissimilar sensors (e.g., the PTS high resolution TV and an IRIS). In order to study the sensitive parameters in existing techniques to accomplish target handoff in the above two cases, the US Army Missile Command, Huntsville, Alabama, let a contract with the Engineering Experiment Station, Auburn University, Auburn, Alabama. This report presents the results of that effort.

Scope of Work

The purpose of this study was to determine the effects of quantization on correlation accuracy for TV and IR digitized scenes. Specifically, the tasks included the following:

a. A simulation will be performed of four TV to IR digitized scenes where the field of view ratios are varied from 2:1 up to 20:1 between the TV to IR imagery. The results of the analysis and simulation will specifically show the sensitivity of handoff system's performance to field of view changes.

b. An analysis and simulation will be performed on the same TV to IR digitized scenes as la to determine effects on target handoff for 4 bit vs 8 bit input imagery quantization. The results should clearly indicate any performance degradation for reduced scene quantization.

Organization of Report

All of the work specified in the Scope of Work has been completed and is documented in this Final Report. Task "a" is reported in Chapter III and Task "b" is reported in Chapter IV. In addition to the specified tasks, a new improved algorithm for TV to TV handoff is presented in Chapter II and its extention to TV to IR handoff is presented in Chapter V. The major conclusions and recommendations are given in Chapter VI.

II. IMPROVED METHOD FOR TV-TO-TV CORRELATION

In TV-to-TV correlation algorithms used previously, the following three quantizers were used to transform digital images to binary form.

1. Line average quantizer
2. Area average quantizer
3. Analog filter as quantizer

For better results using a correlation technique, the K x L reference video and each K x L sub-array of the low-resolution video should have an equal number of zeros and ones while being correlated. That means, each sub-array of LR video should be quantized to an equal number of zeros and ones separately. This requires too much computation and can not be done in real-time with existing hardware.

To overcome the above problem, the three quantizers listed above were used to quantize the digital images to two levels. Equal number of zeros and ones were achieved in the reference by offsetting the level about which the video was quantized. But the LR Video was quantized only once and as a result each K x L sub-array did not have an equal number of zeros and ones. However, the highest peak in the correlation surface was the true peak in most of the simulation runs. In most cases the true peak appeared within the first four peaks. An attempt was made to pull out the true peak and to increase the ratio of the true peak to the next highest peak by correlating the cross correlation surface of HR video and LR video with the autocorrelation surface of

HR video with itself. The correlation of correlation surfaces, however, did not lead to satisfactory performance and was dropped. A new method to bring out the true peak and to increase the ratio of true peak to the next highest peak is discussed below and will be referred to as the improved method.

1. The reference from HR video is correlated with LR video using any of the above preprocessing algorithms (quantization methods).
2. A predetermined number of highest peaks and coordinates of their occurrence are identified from the correlation surface. In this simulation the first four peaks are used because the true peak appears as one of these in all cases.
3. Then the four sub-arrays of the LR digital image corresponding to the four peaks are requantized about their respective means to have an equal number of zeros and ones.
4. The correlation values at those four points are recomputed and the simulation results are tabulated for six different scenes.

Tables 1, 2 and 3 contain the simulation results for a 32 by 32 reference using the line average quantizer, the analog filter quantizer and the area average quantizer respectively. Similar results for a reference array size of 16 x 16 are tabulated in Tables 4, 5 and 6.

In order to implement the above method, one field of LR video has to be stored in memory. Even though it requires additional memory, the following advantages make the improved method worthwhile.

1. Using the improved method on the four sub-arrays of LR video corresponding to the four highest peaks obtained by the initial correlation, yielded the true peak as the highest peak every time when using a 32 by 32 or a 16 by 16 reference array. Cases where the original correlation process yielded a false peak but where the improved method yielded the correct highest peak are marked with an asterisk in Tables 1 through 6. In all but 3 out of the 36 cases the first peak was higher using the improved method.
2. One measure of performance of a correlation technique is the ratio of true peak to the second highest peak. Simulation shows that in all but five of the 36 cases this ratio is considerably higher after using the improved analysis. These ratios before and after the improved analysis are tabulated in Tables 1 through 6.
3. The difference in correlation values between successive peaks increases which indicates better signal-to-noise ratio. Figure 1 shows the plot of first four peaks for 'Jeep in the parking lot' scene using line average quantizer and reference of size 32 x 32, in solid lines. The same plot after improved analysis is drawn in dotted lines.

The improvement in performance is obvious. Notice that the second peak using the original correlation method appears as the third peak after the improved analysis and vice versa.

This can be better understood by referring to Figure 2, which is a plot of the first four peaks before and after improved analysis for the NASA tower scene using a 16 by 16 reference array. The peak is expected

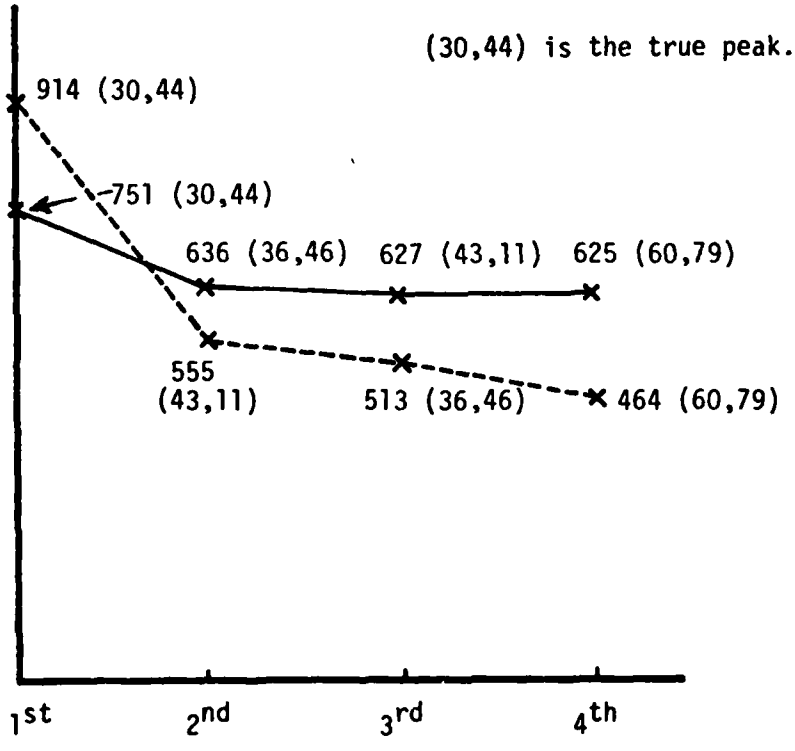

Figure 1. Correlation values of first four peaks before and after improved analysis.

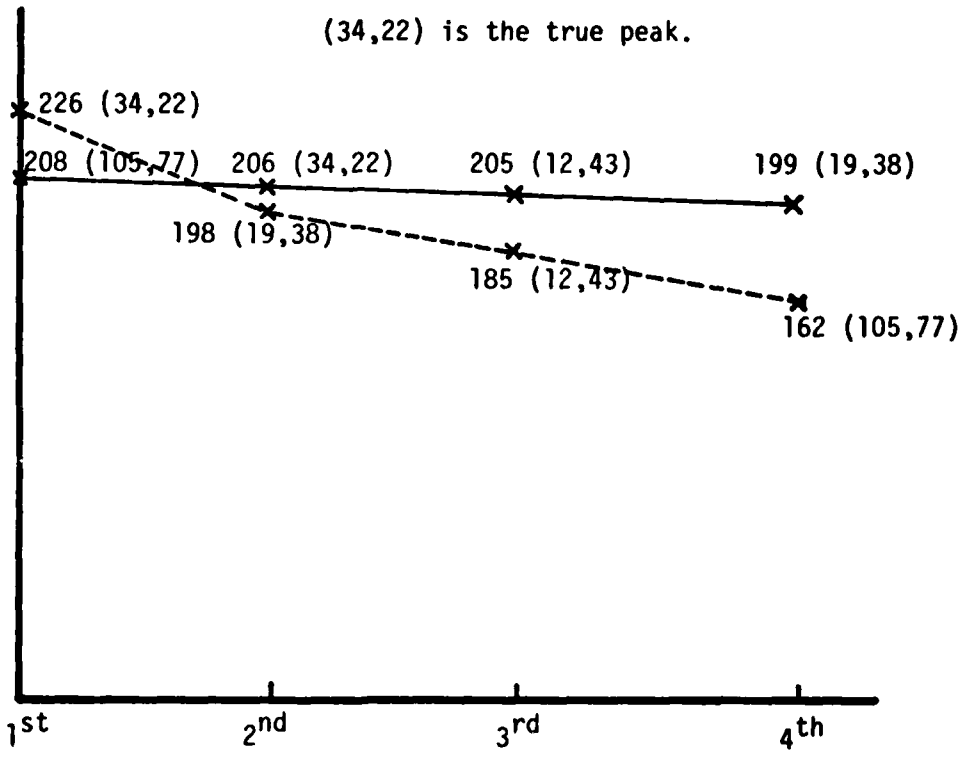

Figure 2. Correlation values of first four peaks before and after improved analysis.

at (33, 21), but when correlated using the line average quantizer, the true peak appears as the second highest peak. The highest peak occurs at (105, 77). The difference between the first and fourth peak is only 9. However, after using the improved method, the true peak appears as the highest peak, with the previous false peak at (105, 77) now being the fourth highest peak. The difference between the first and second peak is 28 and the difference between the first and fourth peak is 64.

A similar analysis was performed using a reference of size 8 x 8. For some scenes the method improved the performance and for others it did not. As concluded before, an 8 x 8 reference array is too small to accomplish correlation. Figures 3 through 8 show plots of the correlation values of the first four peaks before (solid lines) and after (dotted lines) the improved analysis, for all six scenes. Each scene has six cases as explained in Table 7.

From the above simulations and analysis it is concluded that this improved method yields significantly better correlation results than the previously reported correlation methods. It is recommended that MIRADCOM implement this procedure in their TV correlator and test its performance on a large number of typical military scenes.

The improved correlation method consists of the following steps:

1. Perform an initial correlation on one or more video fields using the present method of quantization. Store the last LR field or an average of the last several fields (this tends to help reduce the effects of random noise).

2. For the N highest peaks found in step one above (N can be any predetermined number and was four in the simulations), requantize the LR stored video array about the mean of each K x L subarray at these points where K x L is the size of the reference array. The N highest peaks are found by masking out a region about all previously determined peaks when searching for the next highest peak.

3. Correlate these N K x L requantized subarrays with the K x L reference array. Find the largest of these correlation points and test for goodness of correlation. Steps two and three are not accomplished in real-time but may take several fields. The improved correlation, however, justifies the extra computation time. If time permits a small search about each of these points would further improve the performance.

4. Continue real-time correlation using the method in step one but limit the dynamic search range to some predetermined area about the highest peak as determined in step three. Since a limited dynamic search is conducted, for example a search over a 25 x 25 area rather than the complete 240 x 256 area, a more complex and reliable correlation algorithm could be used because of the extra time available during each 1/60 second correlation cycle.

This method yields a higher probability of finding the true peak and then reduces the possibility of false peaks by limiting the dynamic search range.

Table 1. Line average quantizer with 32 x 32 reference array.

Scene	Method	True Peak	1st Peak	2nd Peak	3rd Peak	4th Peak	Ratio of First Peak to Second Peak
Jeep in front of the fence	Initial	(23,26)	(23,28) 777	(20,23) 667	(77,66) 631	(3, 5) 625	1.2314
	Improved		(23,28) 837	(20,23) 698	(77,66) 560	(3, 5) 623	1.4946
Jeep behind the fence	Initial	(39,37)	(39,37) 743	(27,59) 650	(8,56) 648	(13,30) 640	1.1430
	Improved		(39,37) 898	(13,30) 589	(8,56) 533	(27,59) 432	1.5246
Jeep in parking lot	Initial	(30,44)	(30,44) 751	(36,46) 636	(43,11) 627	(60,79) 625	1.1978
	Improved		(30,44) 914	(43,11) 555	(36,46) 513	(60,79) 464	1.6468
Parking lot	Initial	(28,35)	(28,35) 785	(60,45) 555	-	-	1.1984
	Improved		(28,35) 879	(60,45) 542	-	-	1.6217
NASA tower	Initial	(30,22)	(31,22) 683	(9,41) 648	(16,37) 642	(22,29) 630	1.0540
	Improved		(31,22) 886	(22,29) 841	(16,37) 752	(9,41) 670	1.0535
Water tower	Initial	(33,23)	(32,23) 703	(37,25) 640	(27,26) 615	(49,24) 599	1.1736
	Improved		(32,23) 812	(27,26) 752	(37,25) 679	(49,24) 568	1.4296

Table 2. Analog line average quantizer with 32 x 32 reference array.

Scene	Method	True Peak	1st Peak	2nd Peak	3rd Peak	4th Peak	Ratio of First Peak to Second Peak
Jeep in front of fence	Initial	(23,29)	(24,28) 714	(16,59) 689	(1,70) 687	(59,41) 677	1.0362
	Improved		(24,28) 774	(16,59) 573	(1,70) 517	(59,41) 489	1.3507
Jeep behind the fence	Initial	(39,37)	(19,84)* 763	(39,37) 747	(1,62) 725	(13,22) 724	1.0214
	Improved		(39,37) 875	(1,62) 591	(13,22) 590	(19,84) 515	1.4805
Jeep in parking lot	Initial	(30,54)	(30,53) 839	(44,18) 754	(29,48) 736	(45,75) 730	1.1127
	Improved		(29,48) 821	(30,53) 768	(44,18) 410	(45,75) 350	2.0024
Parking lot	Initial	(28,35)	(28,34) 742	(32, 5) 649	(28,39) 643	(63,71) 642	1.1432
	Improved		(28,34) 871	(28,39) 804	(32, 5) 624	(63,71) 580	1.3958
NASA tower	Initial	(30,32)	(76,89)* 776	(76,82) 765	(81,85) 757	(71,83) 756	1.0143
	Improved		(30,32) 889	(76,89) 597	(76,82) 459	(81,85) 445	1.4891
Water tower	Initial	(33,33)	(33,30) 730	(47,24) 712	(55,24) 664	(11,86) 657	1.0252
	Improved		(33,33) 795	(55,24) 736	(11,86) 593	(47,24) 540	1.0802

Table 3. Area average quantizer with 32 x 32 reference array.

Scene	Method	True Peak	1st Peak	2nd Peak	3rd Peak	4th Peak	Ratio of First Peak to Second Peak
Jeep in front of fence	Initial	(23,26)	(23,28) 790	(25,33) 682	(23,23) 673	(13,55) 650	1.2154
	Improved		(23,28) 897	(23,23) 846	(25,33) 840	(13,55) 670	1.3388
Jeep behind the fence	Initial	(44,42)	(45,42) 800	(45,47) 701	(45,37) 689	(46, 8) 686	1.1662
	Improved		(45,42) 873	(45,47) 817	(45,37) 721	(46, 8) 718	1.2159
Jeep in parking lot	Initial	(25,49)	(24,49) 754	(24,44) 671	(25,27) 664	(10, 6) 653	1.1355
	Improved		(24,49) 914	(24,44) 764	(10, 6) 678	(25,27) 626	1.3481
Parking lot	Initial	(28,35)	(28,36) 810	(28,31) 743	(27,41) 696	(28,24) 693	1.1638
	Improved		(28,36) 862	(28,31) 804	(27,41) 802	(28,24) 751	1.1478
NASA tower	Initial	(25,27)	(26,28) 662	(8,30) 592	(78,75) 589	(26,66) 589	1.1182
	Improved		(26,28) 886	(26,66) 868	(8,30) 807	(78,75) 594	1.0207
Water tower	Initial	(28,28)	(28,27) 683	(50,56) 594	(66,59) 589	(2,50) 585	1.1498
	Improved		(28,28) 795	(50,56) 719	(2,50) 714	(66,59) 681	1.1057

Table 4. Line average quantizer with 16 x 16 reference array.

Scene	Method	True Peak	1st Peak	2nd Peak	3rd Peak	4th Peak	Ratio of First Peak to Second Peak
Jeep in front of the fence	Initial	(37,27)	(38,30) 207	(5,17) 193	(14,40) 192	(94,73) 189	1.0725
	Improved		(38,30) 227	(5,17) 187	(94,73) 139	(14,40) 120	1.2139
Jeep behind the fence	Initial	(47,48)	(47,49) 191	(63,33) 180	(21,43) 175	(6,69) 172	1.0611
	Improved		(47,49) 191	(63,33) 178	(6,69) 172	(21,43) 164	1.0730
Jeep in parking lot	Initial	(41,50)	(40,50) 218	(75,35) 202	(64,30) 197	(53,19) 194	1.0792
	Improved		(40,50) 219	(75,35) 176	(53,19) 175	(64,30) 168	1.2443
Parking lot	Initial	(48,47)	(48,48) 206	(46,22) 196	-	-	1.0510
	Improved		(48,48) 218	(46,22) 144	-	-	1.5138
NASA tower	Initial	(33,21)	(105,77)* 208	(34,22) 206	(12,43) 205	(19,38) 199	1.0097
	Improved		(34,22) 226	(19,38) 198	(12,43) 185	(105,77) 162	1.1414
Water tower	Initial	(37,30)	(37,30) 194	(32,37) 181	(103,48) 180	(28,58) 178	1.0778
	Improved		(37,30) 218	(32,37) 197	(28,58) 191	(103,48) 141	1.1414

Table 5. Analog line average quantizer with 16 x 16 reference array.

Scene	Method	True Peak	1st Peak	2nd Peak	3rd Peak	4th Peak	Ratio of First Peak to Second Peak
Jeep in front of fence	Initial	(37,37)	(14,78)* 191	(38,38) 188	(43,44) 186	(29,60) 185	1.0160
	Improved		(38,38) 226	(29,60) 162	(43,44) 148	(14,78) 126	1.3950
Jeep behind the fence	Initial	(47,48)	(47,49) 215	(61,16) 206	(94,101) 197	(39,80) 196	1.0436
	Improved		(47,49) 172	(61,16) 151	(39,80) 114	(94,101) 100	1.1391
Jeep in parking lot	Initial	(41,60)	(41,60) 215	(76,45) 209	(17,24) 192	(25,90) 189	1.0287
	Improved		(41,60) 229	(76,45) 183	(17,24) 155	(25,90) 112	1.2514
Parking lot	Initial	(28,35)	(30,16)* 201	(47,85) 197	(13,23) 193	(47,90) 192	1.0203
	Improved		(28,35) 224	(30,16) 173	(13,23) 154	(47,85) 114	1.2947
NASA tower	Initial	(33,32)	(102,86)* 239	(97,88) 232	(71,89) 232	(28,34) 220	1.0302
	Improved		(33,32) 217	(97,88) 193	(102,86) 187	(71,89) 152	1.1243
Water tower	Initial	(37,40)	(37,35)* 197	(37,40) 192	(33,48) 183	(28,64) 175	1.0103
	Improved		(37,40) 218	(37,35) 204	(33,48) 192	(28,64) 187	1.1658

Table 6. Area average quantizer with 16 x 16 reference array.

Scene	Method	True Peak	1st Peak	2nd Peak	3rd Peak	4th Peak	Ratio of First Peak to Second Peak
Jeep in front of fence	Initial	(32,32)	(33,35) 223	(23,61) 205	(34,40) 196	(23,45) 195	1.0878
	Improved		(33,35) 227	(23,61) 187	(33,40) 186	(23,45) 167	1.2139
Jeep behind the fence	Initial	(52,53)	(53,54) 201	(40,43) 192	(28, 8) 179	(54,26) 178	1.0468
	Improved		(53,54) 207	(40,43) 186	(54,26) 175	(28, 8) 167	1.1129
Jeep in parking lot	Initial	(36,55)	(36,55) 213	(13,67) 193	(12,59) 189	(13,75) 187	1.1036
	Improved		(36,55) 229	(13,75) 175	(13,67) 172	(12,59) 167	1.3085
Parking lot	Initial	(28,35)	(28,36) 216	(40,68) 203	(28,31) 200	(47,85) 198	1.0640
	Improved		(28,36) 232	(28,31) 212	(47,85) 158	(40,68) 152	1.4684
NASA tower	Initial	(28,27)	(29,28) 189	(92,62) 175	(27,91) 171	(27,42) 170	1.0800
	Improved		(29,28) 220	(27,96) 212	(27,42) 180	(92,62) 89	1.0377
Water tower	Initial	(32,35)	(32,34) 179	(8,23) 177	(54,83) 173	(53,68) 170	1.0112
	Improved		(32,34) 218	(53,68) 166	(8,23) 157	(54,83) 139	1.3132

Table 7. Details of figures 3 through 8.

Section	Size of Reference	Quantizer Used in Initial Correlation Process
a	32 x 32	Line average quantizer
b	32 x 32	Analog filter quantizer
c	32 x 32	Area average quantizer
d	16 x 16	Line average quantizer
e	16 x 16	Analog filter quantizer
f	16 x 16	Area average quantizer

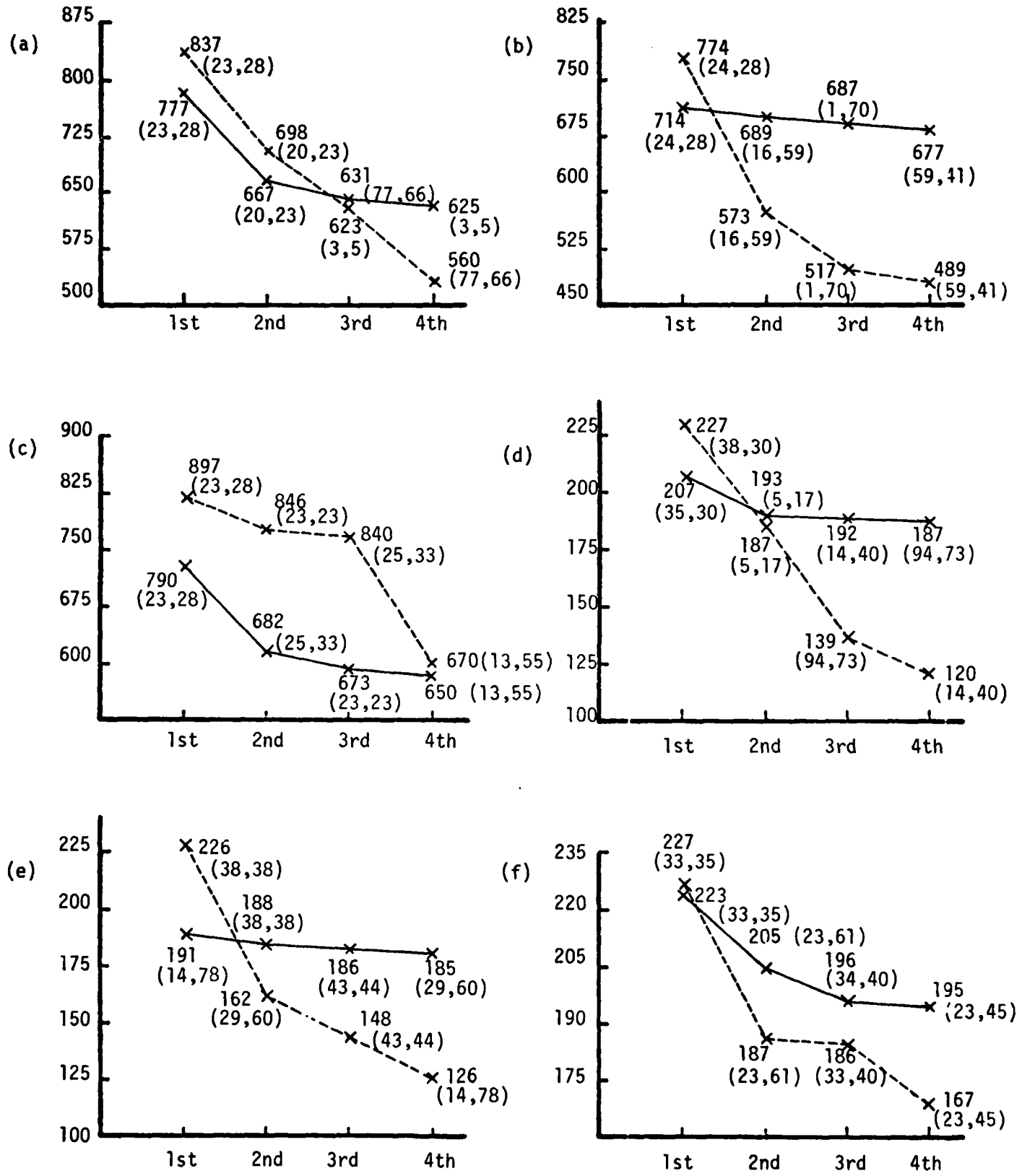

Figure 3. Correlation values of first four peaks before and after improved analysis for jeep in front of the fence.

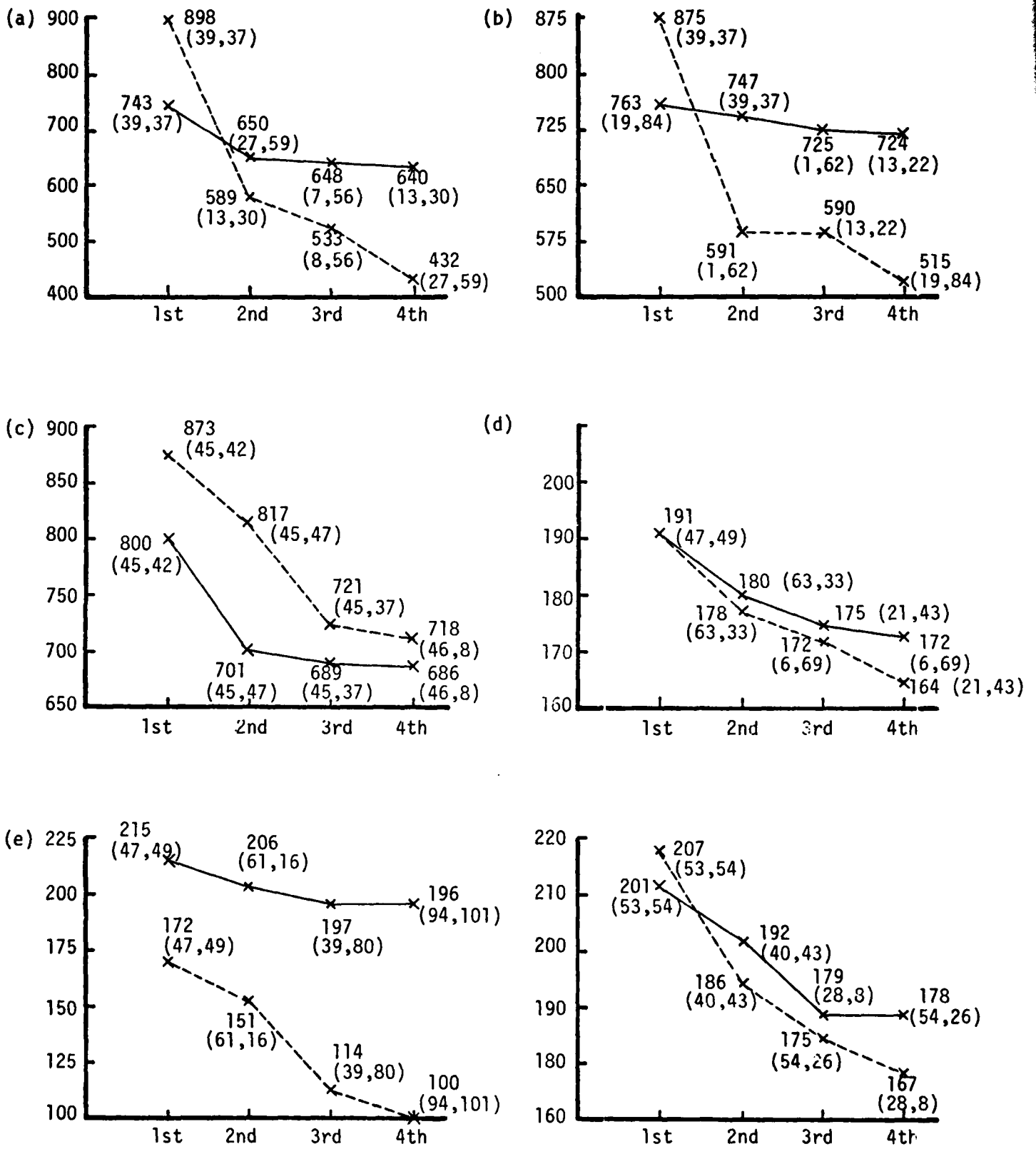

Figure 4. Correlation values of first four peaks before and after improved analysis for jeep behind the fence.

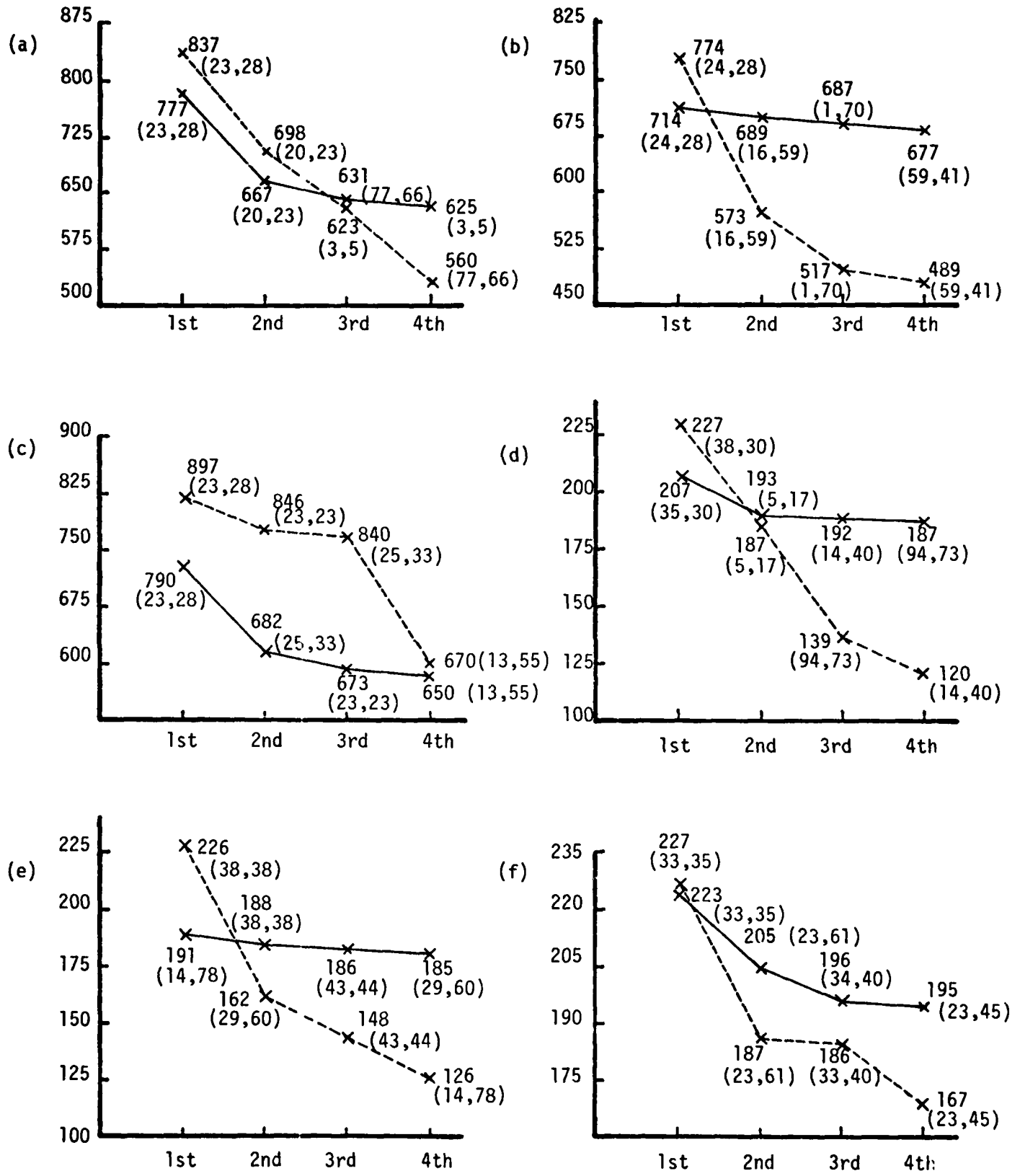

Figure 3. Correlation values of first four peaks before and after improved analysis for jeep in front of the fence.

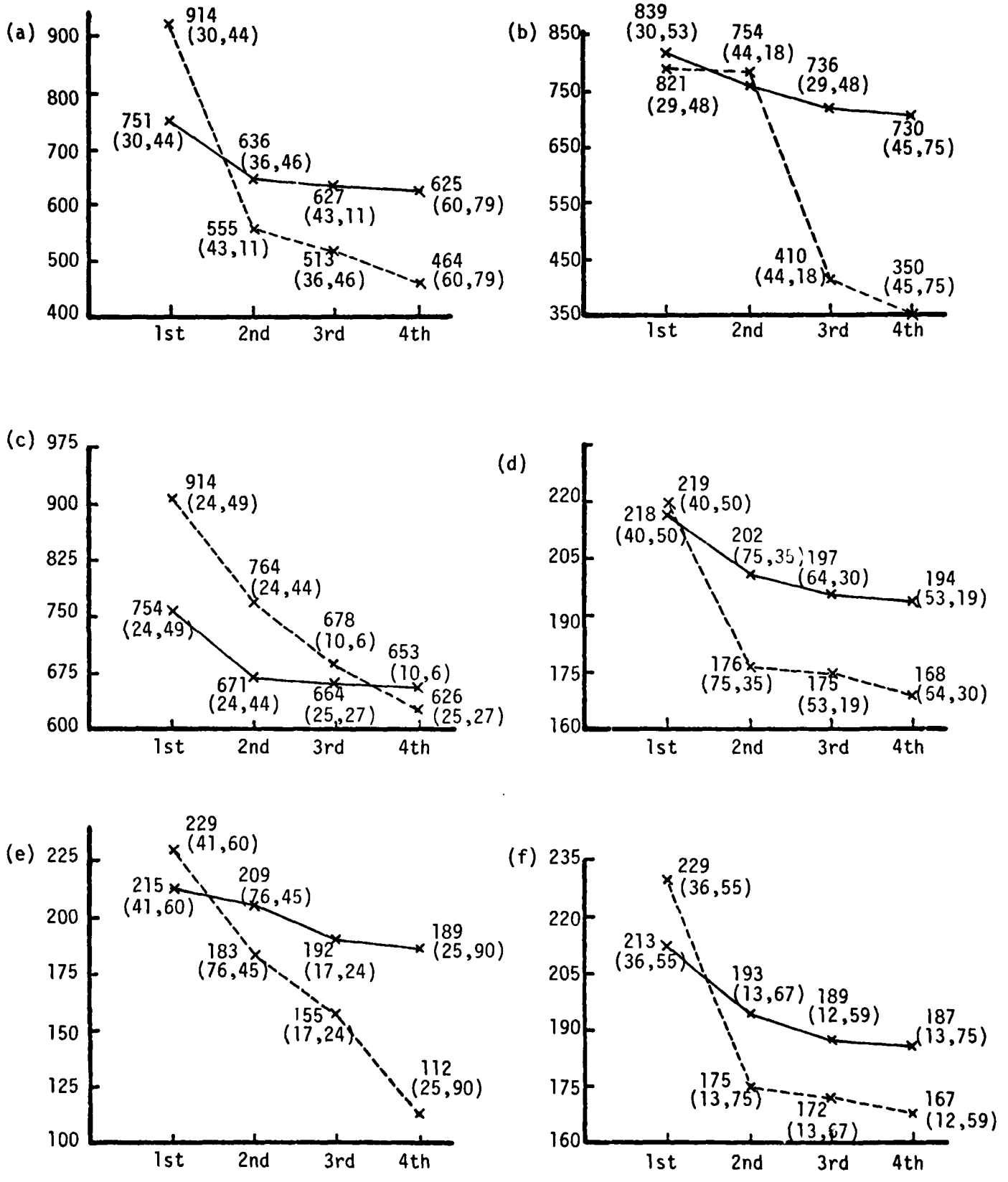

Figure 5. Correlation values of first four peaks before and after improved analysis for jeep in the parking lot.

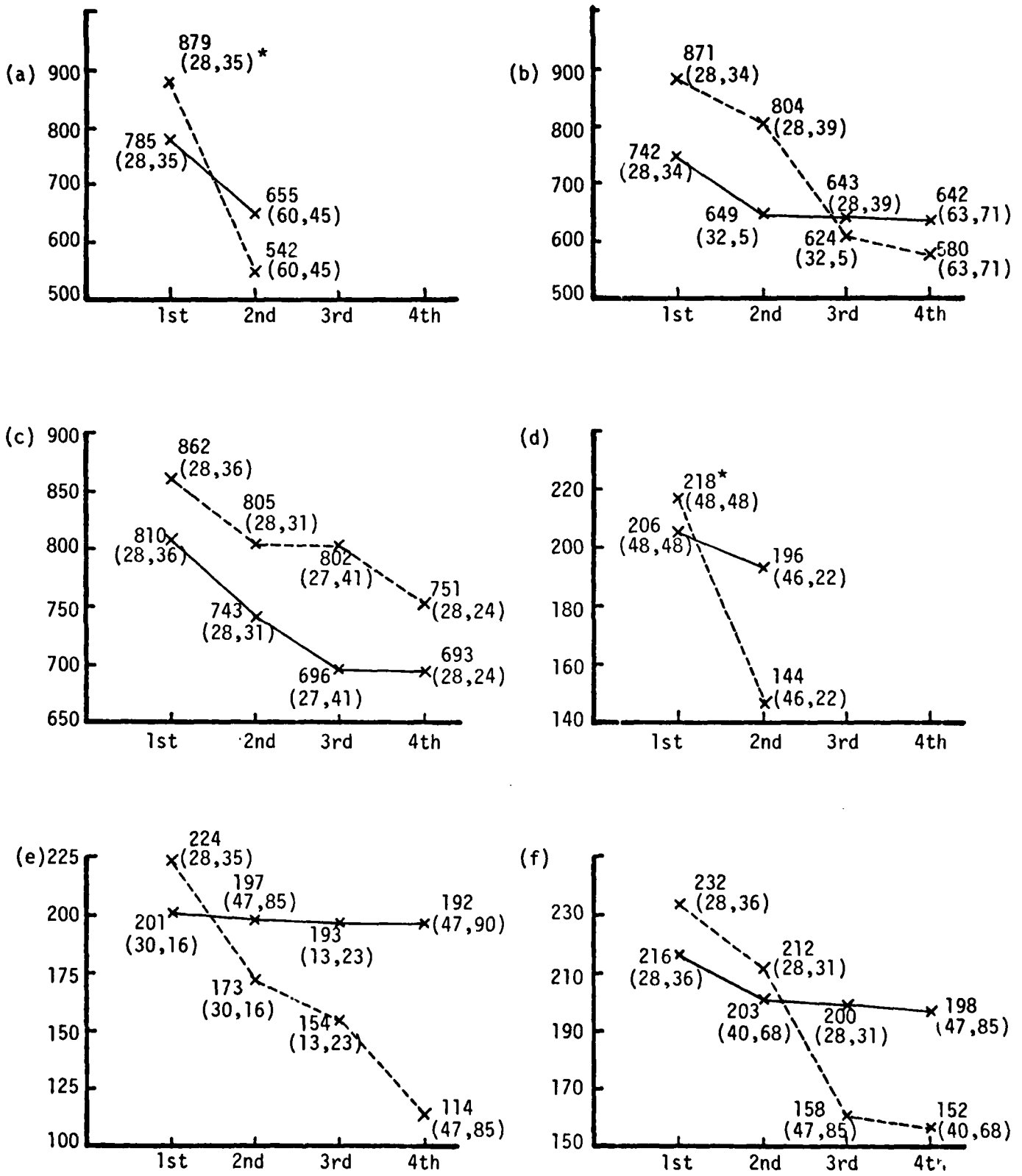

Figure 6. Correlation values of first four peaks before and after improved analysis for parking lot scene.

*3rd and 4th peaks are not obtained.

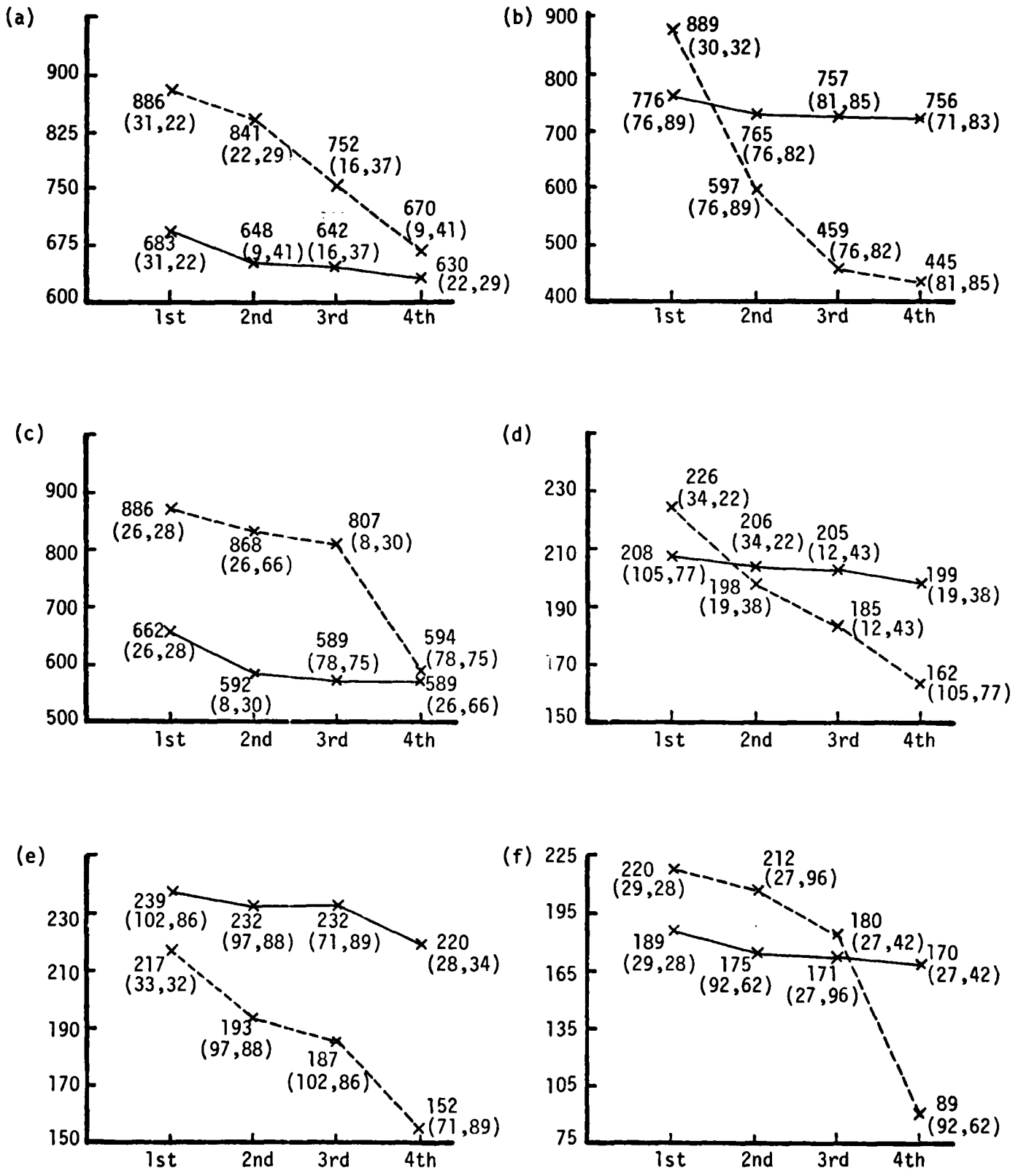

Figure 7. Correlation values of first four peaks before and after improved analysis for NASA tower scene.

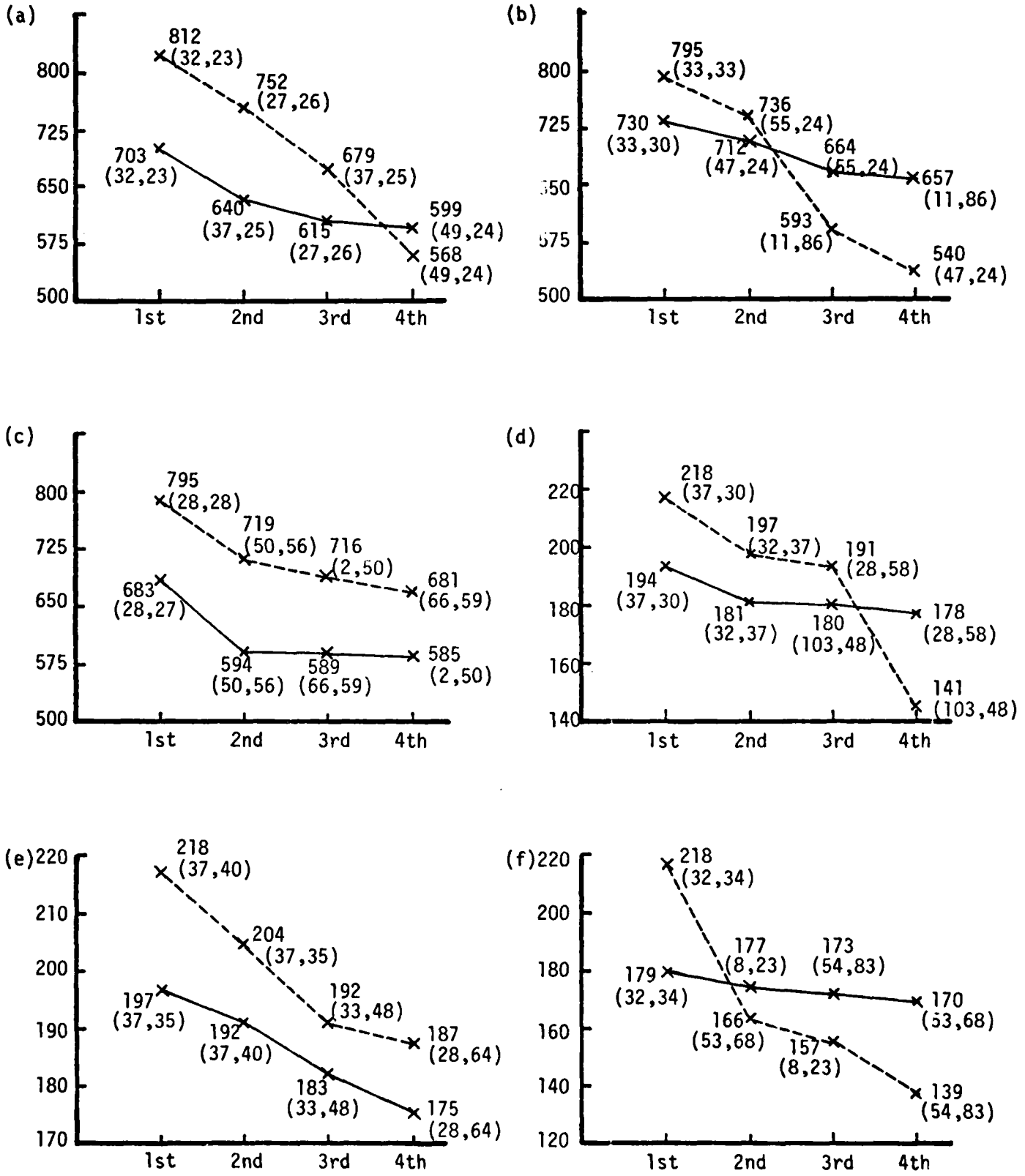

Figure 8. Correlation values of first four peaks before and after improved analysis for water tank scene.

III. TV-TO-IR CORRELATION ALGORITHM

In this chapter preprocessing algorithms used to transform high resolution TV digital images and low resolution IR digital images to binary form are presented along with the correlation results. In order for the correlation of binary images to be a valid measure of similarity the following two conditions must be satisfied.

1. The two videos being correlated must have the same spatial resolution.
2. When HR and LR images are obtained from sensors operating in different frequency spectra, the preprocessing and quantization process must yield binary arrays based on similar measures of scene content.

Equalization of Spatial Resolutions of HR and LR Videos

The difference in resolution of HR and LR videos is caused by the differing fields of view, number of IR detections and TV lines per frame, frame rate, aspect ratio and sampling rate of the two sensor systems. The resolutions of the two videos are equalized in the following way.

1. The size of the unprocessed low resolution IRIS video array is 240 x 512. A sampling rate of 10Mhz was used to obtain this array. Taking every other column effectively reduces the sampling rate to 5MHz. Every third row of this array is used since each

detector is read out three times in the IRIS in order to get the data into standard video format. This reduced array, ULRV, is therefore of size 80 x 256.

2. The size of the high resolution TV image is 240 x 512. By selecting every other column of this image the sampling rate is effectively reduced to 5MHz yielding a 240 x 256 pixel image, UHRV. The vertical scale factor, W_V, and horizontal scale factor, W_H, were determined through extensive simulation to be 13.48 and 4.5, respectively. When the UHRV array is reduced using the above scale factors, the pixel resolution of the reduced high resolution video (RHRV of size 17 x 56) is identical to that of ULRV.

Edge Extraction

In order for the correlation of binary images to be a valid measure of similarity it is necessary that the quantization process be based on a similar measure of scene content. For the case in which the images to be correlated are obtained from sensors operating in different frequency spectra, quantization based on line average or area average of the video amplitude no longer supplies similar binary images to the correlator. Therefore some other measure on which quantization is based must be used when correlating images from dissimilar sensors. One such measure is the edge content in the two images. All edge detection schemes base their decision on the gradient value associated with a particular pixel in the image. Pixels exhibiting a high gradient value as compared to a threshold are considered to be edge points and those pixels with a low gradient value are considered to be non-edge points.

The Sobel edge detector is used to compute the gradient magnitudes of pixels in this report. This method estimates the gradient magnitude at a particular pixel based on the eight nearest pixels surrounding the pixel of interest. Figure 9 illustrates a 3 x 3 pixel array used to estimate the gradient magnitude at pixel (i,j).

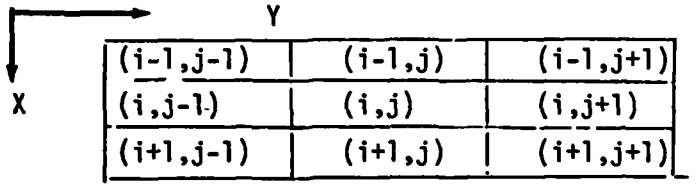

Figure 9. Layout for the estimation of gradient value associated with pixel (i,j).

Figure 10 illustrates the Sobel set of weighting matrices used for gradient estimation.

$$W_1 = \begin{bmatrix} 1 & 2 & 1 \\ 0 & 0 & 0 \\ -1 & -2 & -1 \end{bmatrix} \qquad W_2 = \begin{bmatrix} 1 & 0 & -1 \\ 2 & 0 & -2 \\ 1 & 0 & -1 \end{bmatrix}$$

Figure 10. Weighting matrices for Sobel edge detector.

The Gradient along the x-axis is referred to as $S_x(i,j)$ and is given by

$$S_x(i,j) = \sum_{K=1}^{3} \sum_{L=1}^{3} G(i+K-2,j+L-2)\, W_1(K,L) \qquad (1)$$

The Gradient along the y-axis is $S_y(i,j)$ and is given by

$$S_y(i,j) = \sum_{K=1}^{3} \sum_{L=1}^{3} G(i+K-2,j+L-2)\, W_2(K,L) \quad . \qquad (2)$$

Then the total gradient magnitude associated with pixel (i,j) is given by

$$||\nabla g(i,j)|| = [S_x^2(i,j) + S_y^2(i,j)]^{1/2} \quad . \qquad (3)$$

A more computationally efficient algorithm is given by Equation 4.

$$G(i,j) = |S_x(i,j)| + |S_y(i,j)| \quad (4)$$

It is easy to see that, if the original image is of size NxM, the gradient image will be of size (N-2) x (M-2). The reduction of array size presents no problem in the correlation system. GLRV and GHRV are the gradient images of ULRV and RHRV respecively obtained by using the Sobel edge detector. These gradient images are quantized to two levels based on a threshold, thus creating the binary images which are correlated. The problem of choosing the quantization threshold is addressed later in this chapter.

Sensitivity of Correlator to Field of View Errors

In order to correlate two videos, they must have the same spatial resolution. In order to equalize the resolution of high resolution TV video and low resolution IR video, a vertical scale factor W_V equal 13.48 and horizontal scale factor W_H equal 4.5 were used. In order to study the effect of scale factor errors, simulation was performed on the NASA tower and parking lot scenes with different values of W_H AND W_V. Simulation results with errors of -10%, -5%, +5% and +10% from the originally chosen values of W_H and W_V are presented in Tables 8 and 9. For the NASA tower the true peak appeared within the first four peaks for all cases. The Parking lot scene worked in 3 out of 5 cases. From this result along with other simulation, it is concluded that WH equal 4.5 and WV equal 13.48 are the correct scale factors and are used for resolution reduction for the work reported here.

Table 8. Scene - NASA Tower.

Horizontal and Vertical Scale Factors	Threshold	Expected Peak	1st Highest Peak	Average Value of Corr. Surface	Standard Deviation of Corr. Surface	S/N Ratio	2nd Highest Peak	3rd Highest Peak	4th Highest Peak
WH= 4.05	80		683				676	662	652
WV=12.132		(39,102)	(37,103)	505.023	49.836	3.571	(37,108)	(37,113)	(37, 98)
WH= 4.275			597				589	577	570
WV=12.806	80	(40,103)	(37,110)	444.763	45.390	3.354	(38,103)	(37,115)	(37, 84)
WH= 4.5		(40,104)	555				550	540	536
WV=13.48	80		(38,111)	395.552	43.058	3.703	(38,105)	(38,119)	(38,100)
WH= 4.725		(40,105)	508	356.645	37.796	4.005	498	491	489
WV=14.554	80		(38,108)				(38,120)	(38,113)	(38,103)
WH= 4.95		(41,106)	450				444	431	426
WV=15.228	80		(39,120)	313.278	33.266	4.110	(39,108)	(39,113)	(39,102)

Table 9. Scene - Parking lot.

Horizontal and Vertical Scale Factors	Threshold	Expected Peak	1st Highest Peak	Average Value of Corr. Surface	Standard Deviation of Corr. Surface	S/N Ratio	2nd Highest Peak	3rd Highest Peak	4th Highest Peak
WH= 4.05 WV=12.132	150	(34,67)	701 (41,121)	525.914	48.430	3.615	685 (41,127)	678 (41,138)	676 (35, 47)
WH= 4.275 WV=12.806	150	(35,67)	612 (35, 51)	461.546	44.410	3.388	610 (41,122)	609 (41,128)	600 (42,133)
WH= 4.5 WV=13.48	150	(35,67)	559 (35, 66)	410.074	39.832	3.739	557 (42,133)	552 (42, 42)	548 (42,128)
WH= 4.725 WV=14.554	150	(35,67)	508 (36, 65)	367.727	34.767	4.035	492 (36, 60)	490 (43, 83)	485 (42,132)
WH= 4.95 WV=15.228	150	(36,67)	447 (36, 66)	321.710	30.524	4.105	441 (36, 50)	438 (36, 58)	436 (43,100)

Effect of Threshold on Correlation Process

Pixels in the gradient image corresponding to edge points exhibit a high gradient value and pixels corresponding to non-edge points exhibit a low gradient value. In order to quantize edge points to ones and nonedge points to zeros a proper threshold should be chosen. To investigate the effect of the gradient threshold on correlation accuracy, the parking lot scene was simulated for different values of threshold as explained below.

1. The gradient image of the reference video GHRV is quantized to yield an equal number of zeros and ones.

2. The quantization process used to quantize the gradient image GLRV is given by Equation 5.

$$GLRV(I,J) = \begin{cases} 1 & \text{if } GLRV(I,J) \geq T \\ 0 & \text{otherwise} \end{cases} . \qquad (5)$$

where T is the threshold.

T is varied from 50 to 150 and the results are tabulated in Table 10. Coordinates of the expected peak in the correlation surface are calculated by visual inspection of overstruck images of RHRV and ULRV.

From Table 10, it can be seen that the true peak does not appear within the first four highest peaks in the Correlation Surface when T is between 50 and 100. When T equals 130, the true peak appears as the fourth highest peak. When T equals 150, true peak appears as the highest peak in the correlation surface. This simulation along with the simulation of other scenes leads to the following conclusions.

Table 10. Effect of threshold on correlation process for parking lot scene.

Threshold	Expected Peak	1st Highest Peak	Average Value of Corr. Surface	Standard Deviation of Corr. Surface	S/N Ratio	2nd Highest Peak	3rd Highest Peak	4th Highest Peak
T= 50	(35,67)	(43, 81) 505	410.251	29.736	3.186	(41,121) 500	(42,145) 499	(44, 73) 498
T= 70	(35,67)	(43, 87) 545	412.397	37.595	3.527	(44, 62) 539	(43, 81) 536	(43,105) 534
T= 90	(35,67)	(43, 87) 560	412.600	40.602	3.630	(43, 81) 556	(42,144) 555	(42,133) 554
T=100	(35,67)	(43, 85) 567	412.197	41.369	3.742	(42,145) 562	(42,133) 561	(43, 80) 557
T=130	(35,67)	(42,133) 562	410.499	41.465	3.654	(43, 83) 557	(42,143) 557	(35, 66) 552
T=150	(35,67)	(35, 66) 559	410.074	39.832	3.739	(42,133) 557	(42,142) 552	(42,128) 548

1. There is a range of values for Threshold T which leads to proper correlation. However, it is not possible to have a single value of T which will work for all scenes. Threshold value is scene dependent and also depends on the sharpness of edge points.
2. Too low a value of T results in a large number of ones in the binary image which leads to false peaks in the correlation process.
3. Similarly, a high threshold value results in a larger number of zeros in the binary image which in turn causes false peaks in the correlation surface.
4. Therefore, choosing the proper threshold for each scene is critical. A means of estimating the threshold based on some characteristics of the gradient array should be used. In the following section some of the methods tried to estimate the threshold automatically are presented.

Automatic threshold and quantization

In this section three methods of automatically setting the quantization thresholds for the gradient arrays are discussed.

1. Choosing threshold by intuition

Let TL and TH represent the threshold for GLRV and GHRV, respectively. TL and TH are chosen such that only the dominant edges in both low resolution and high resolution videos are quantized to ones as given in Equations 6 and 7.

$$GLRV(I,J) = \begin{cases} 1 & \text{if } GLRV(I,J) \geq TL \\ 0 & \text{if otherwise} \end{cases} \quad (6)$$

$$GHRV(I,J) = \begin{cases} 1 & \text{if } GHRV(I,J) \geq TH \\ 0 & \text{if otherwise} \end{cases} \quad (7)$$

That means the binary images will have a relatively small number of ones when compared to the number of zeros. As a result the large number of zeros can cause false peaks as explained in the previous section. In order to avoid this problem, only edge points of the reference video are correlated with the live video. Non-edge points are ignored. This can be easily done by correlating only ones of the reference with the live binary image. The correlation value R(I,J) at the point (I,J) in the Correlation Surface is the number of times the following equations are both satisfied.

$$GHRV(i,j) = GLRV(I+i-1,J+j-1) \quad (8)$$

for $i = 1, 2, \ldots K$, $j = 1, 2, \ldots L$

if reference is of size K by L

$$GHRV(i,j) = 1 \quad (9)$$

2. Area average method

The gradient images GLRV and GHRV obtained by using the Sobel edge detector are quantized to two levels based on the average pixel value of nine pixels centered about the pixel to be quantized as given in Equation 10. Figure 11 shows the layout for quantizing pixel GLRV(I,J).

$$AVG = \frac{1}{9} \sum_{i=I-1}^{I+1} \sum_{j=J-1}^{J+1} GLRV(i,j) \quad (10)$$

The quantization process is now given by Equation 11.

$$GLRV(I,J) = \begin{cases} 1 & \text{if } GLRV(I,J) \geq SL \times AVG \\ 0 & \text{if otherwise} \end{cases} \quad (11)$$

where SL is the threshold scaling factor. A low value of SL yields fat edges and a high value yields fine edges. This type of defocusing masks (3 x 3 or 5 x 5) have been used for obtaining local threshold values in edge detection before. Gunner Robinsons's [1] method of detecting edges is similar to the one explained in this section. Robinson computed the local threshold for point (I,J) using equation 12.

$$T = \frac{1}{16} \begin{bmatrix} 1 & 2 & 1 \\ 2 & 4 & 2 \\ 1 & 2 & 1 \end{bmatrix} \begin{bmatrix} X(I-1,J-1) & X(I-1,J) & X(I-1,J+1) \\ X(I,J-1) & X(I,J) & X(I,J+1) \\ X(I+1,J-1) & X(I+1,J) & X(I+1,J+1) \end{bmatrix} \quad (12)$$

where X is the gradient array.

Point (I,J) is classified as edge or non-edge point based on this local threshold T along with a connectivity test.

Quantization of GHRV is similar to that of GLRV with SH as the scaling factor. Simulation results with SL and SH equal 1.0 to 1.4 are presented in a later section.

(I-1,J-1)	(I-1,J)	(I-1,J+1)
(I,J-1)	(I,J)	(I,J+1)
(I+1,J-1)	(I+1,J)	(I+1,J+1)

Figure 11. Layout for the quantization of GLRV(I,J).

3. Quantization based on mean and standard deviation of gradient images

In this method, the mean and standard deviation are computed for GLRV and GHRV. Let,

μ_L = mean of GLRV

μ_H = mean of GHRV

σ_L = standard deviation of GLRV

σ_H = standard deviation of GHRV

Thresholds THL and THH for GHRV are computed and shown by Equations 13 and 14.

$$THL = \mu_H - S\,\sigma_H \tag{13}$$

$$THH = \mu_H + S\,\sigma_H \tag{14}$$

where S is a scaling factor ≥ 0.

The quantization process for GHRV is given by Equation 15.

$$GHRV(I,J) = \begin{cases} 1 & \text{if } GHRV(I,J) \geq THH \\ 0 & \text{if } GHRV(I,J) \leq THL \end{cases} \tag{15}$$

Pixels of GHRV with values between THL and THH are don't cares and are not considered in the correlation process. The quantization procedure for GLRV is similar to that of GHRV. Figure 12 illustrates the entire process for S = 0, 0.2, 0.4 and 0.5.

After transforming ULRV and RHRV to GLRV and GHRV, correlation is accomplished as follows. The correlation value R(I,J) at the point (I,J) in the correlation surface is the number of times the following equations are both satisfied.

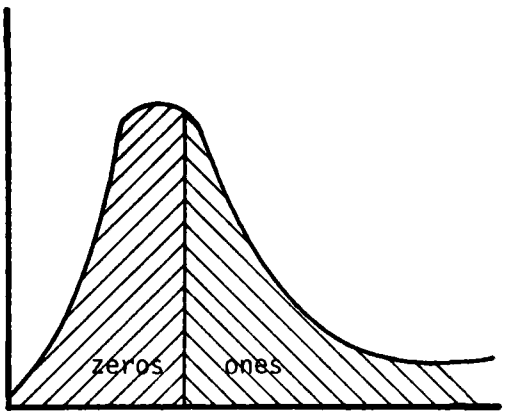

μ_H

(a) S=0. THL = THH = μ_H

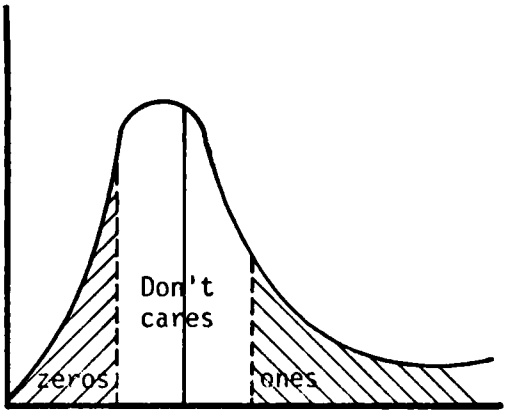

$\mu_H-0.2\sigma_H$ μ_H $\mu_H+0.2\sigma_H$

(b) S = 0 • 2
THL = μ_H = $0.2\sigma_H$
THH = μ_H + $0.2\sigma_H$

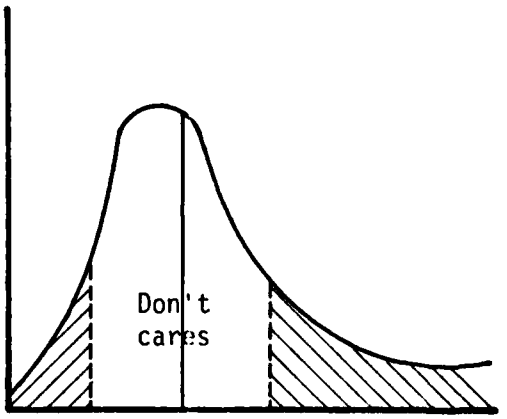

$\mu_H-0.4\sigma_H$ μ_H $\mu_H+0.4\sigma_H$

(c) S = 0.4

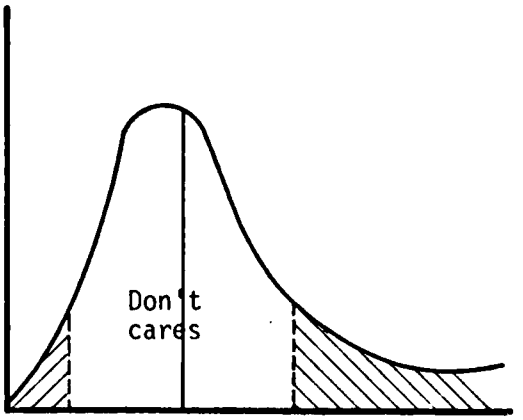

$\mu_H-0.5\sigma_H$ μ_H $\mu_H+0.5\sigma_H$

(d) S = 0.5

Figure 12. Pictorial representation of quantization process.

$$GHRV(i,j) \leq 1 \tag{16}$$

$$GHRV(i,j) = GLRV(I+i-1,\ J+j-1) \tag{17}$$

for i = 1, 2, ... K

j = 1, 2, ... L

if GHRV is of size K by L.

Since the don't cares have gradient value greater than 1, the above method deletes them from being correlated. Simulation results for all scenes considered are presented in the next section on a scene by scene basis.

TV-to-IR Correlation Simulation

The three methods used in the simulations reported in this section are listed in Table 11.

Scene 1 - NASA Tower

Simulation results for NASA tower using the various methods discussed in the last section are presented in Table 12. Some of the features and observations are listed below for convenience.

1. When correlated by method one with TL equal 150 and TH equal 150, the true peak appeared as the highest peak and the S/N ratio was 3.963. When TL and TH are increased to 200, the true peak again appeared as the highest peak and the S/N ratio increased from 3.963 to 5.316. The S/N ratio is defined to be

$$S/N = \frac{\text{Peak value - Corr. sur. avg. value}}{\text{standard deviation of corr. sur.}} \tag{18}$$

The second highest peak in all cases was obtained by masking out a 9 x 9 pixel area centered at the highest peak and searching the

remaining array for its highest peak. The third highest peak was obtained by masking out a 9 x 9 array about the first and second peak. The fourth was obtained similarly. Note from Table 12 with TL=TH=150 using method 1 the four highest peaks are at (38,106), (38,111), (41,82) and (41,93), respectively. These are all part of the correlation surface close to the true peak. This indicates that the true peak is rather wide and that the second highest peak in the correlation surface is less than 100.

2. When correlated using the area average method to quantize GLRV and GHRV the results were as follows.

(a) With SL equal to 1.0 and SH equal to 1.0, the true peak appears as the second highest peak with a S/N ratio of 4.125 (both ones and zeros were correlated). Note, however, that the first three peaks are all part of the correlation peak located at the true correlation point.

(b) With SL equal to 1.0 and SH equal to 1.4, the true peak appears as the third highest peak with a S/N ratio of 4.686 (both zeros and ones were correlated). The same note as in (a) applies here also.

(c) When edge points only are correlated with SL equal to 1 and SH equal to 1.4 the true peak appears as the highest peak with a S/N ratio of 4.398.

3. When correlated using the third method based on mean and standard deviation of gradient images, the results were as follows.

(a) With S=0, 0.2 and 0.5, the true peak appeared as second highest peak in the correlation surface. Note, however, that the first three peaks are a part of the same overall correlation surface peak area.

(b) With S = 0.4, the true peak appeared as third highest peak which was a part of the ture peak in the correlation surface. The S/N ratio increased as S is increased from 0 to 0.5.

Scene 2 - Parking lot

Simulation results for the parking lot scene are presented in Table 13.

1. When correlated using the first method with TL equal to 150 and TH equal to 150, the true peak appeared as the highest peak and the S/N ratio was 2.879. When TL and TH are increased to 200, the true peak appeared as the highest peak and the S/N ratio increased from 2.879 to 3.541.

2. When correlated using area average method to quantize GLRV and GHRV, the results were as follows.

(a) With SL equal to 1.0 and SH equal to 1.0, the highest peak occurred at the expected coordinate with the S/N ratio equal to 5.015 (both zeros and ones are correlated).

(b) With SL equal to 1.0 and SH equal to 1.4, the highest peak in the correlation surface was again at the expected coordinates and the S/N ratio dropped from 5.015 to 3.813 (both zeros and ones are correlated).

(c) With SL equal to 1.0, SH equal to 1.4 and edge points only were correlated, the true peak appeared as highest peak and S/N ratio was 4.161.

3. When correlated using method 3 based on mean and standard deviation of gradient images, the results were as follows.

(a) With S equal to 0.0, the true peak appeared as the fourth highest

peak in the correlation surface. With S equal to 0.2 the true peak did not appear in the first four peaks.

(b) With S equal to 0.4 and .5 the true peak appeared as the highest peak in the correlation surface. The S/N ratio increased as S was increased from 0 to 0.5.

Scene 3 - Water tank

The simulation results for the water tower scene are given in Table 14 and summarized below.

1. When correlated using the first method, none of the four peaks appeared at the expected coordinates in the correlation surface. Changing the threshold to other values also did not lead to correct correlations.

2. The area average method also failed to yield a valid correlation.

3. Results obtained using method three based on mean and standard deviation of gradient images was better than the first and second methods.

(a) When each gradient image was quantized about its mean, the true peak did not appear within the first four peaks.

(b) When S = 0.2, the correlation value at the expected coordinates was the third highest peak in the correlation surface.

(c) When S = 0.4 and S = 0.5, the true peaks appeared as the highest peaks in the correlation surfaces. The S/N ratio was 3.208 when S = 0.4 and 3.694 when S = 0.5.

Scene 4 - Rock quarry

Simulation results for rock quarry scene are tabulated in Table 15.

1. The results using methods 1, 2(a), and 2(b) were completely unsatisfactory.

2. However, method three based on mean and standard deviation worked better. For values of S equal to 0, 0.2 and 0.5, the true peaks appeared as the highest peak in their respective correlation surfaces. When S equals 0.4, the true peak appeared as the second highest peak in the correlation surface but was within five pixels of the first peak. This was considered to be a successful correlation. The S/N ratio increased as S is increased from 0 to 0.5.

Comparison of the Four Methods

1. The first method gave satisfactory results for two scenes (NASA tower and Parking lot) and did not give good results for the other two scenes. The S/N ratio increased as TL and TH were increased. The rock quarry and water tank scenes may have worked for some other values of TL and TH, but it was not possible to try many values for TL and TH due to computational limitations. However, various values for TL and TH ranging from 50 to 250 were tried. Therefore it can be concluded that optimum values for TL and TH to ensure proper correlation are scene dependent and the first method is not practical for a real-time system.

2. Methods 2(a) and 2(b) based on local area average of gradient image gave satisfactory results for the NASA tower and parking lot scenes. The true peak appeared within the first four peaks for the NASA tower scene for all cases tried. The true peak always appeared as

the highest peak in the correlation surface for the parking lot scene. However, this method completely failed to identify targets in case of the water tower and rock quarry scenes. Still, this method can be considered superior to the first method due to the fact that one does not have to guess threshold.

3. The performance of method three based on the mean and standard deviation of the gradient images is better than that of the first three methods. This method was tried with values of 0, 0.2, 0.4 and 0.5 for S. The true peak appeared within the first four peaks in each of four trials for the NASA tower, parking lot and rock quarry scenes. In all simulations except the one for which S equals 0, the true peak appeared within the four highest peaks for the water tank scene. This method, however, involves more computation due to the fact that the mean and standard deviation must be computed for GLRV as well as for the reference array from GHRV.

Table 11. Correlation methods used in Tables 12 through 23.

Method 1	-	Threshold by intuition or trial-and-error
Method 2(a)	-	Threshold obtained by averaging a 3 x 3 pixel area around pixel to be quantized as defined by Equations 8 and 9. All pixels in the K x L reference array are used in the correlation algorithm.
Method 2(b)	-	Same as Method 2 except only edge points (ones) in the reference array are used in the correlation algorithm.
Method 3	-	Threshold for quantization based on the mean and standard deviation of the gradient arrays.

Table 12. NASA tower TV-to-IR correlation.

Method	Threshold	Expected Peak	1st Highest Peak	Average Value of Corr. Surface	Standard Deviation of Corr. Surface	S/N Ratio	2nd Highest Peak	3rd Highest Peak	4th Highest Peak
1	TL=150 TH=150	(40,104)	111 (38,106)	16.983	23.725	3.963	104 (38,111)	103 (41, 82)	100 (41, 93)
	TL=200 TH=200	(40,104)	78 (38,106)	7.601	13.243	5.316	72 (41, 94)	71 (41, 88)	69 (39, 76)
2(a)	SL=1.0 SH=1.0	(40,104)	409 (38,120)	340.072	16.351	4.215	400 (39,107)	400 (36, 91)	396 (59, 11)
	SL=1.0 SH=1.4	(40,104)	415 (38,121)	352.520	12.908	4.686	414 (38,113)	409 (39,107)	402 (33,118)
2(b)	SL=1.0 SH=1.4	(40,104)	44 (39,107)	24.527	4.428	4.398	42 (39, 78)	41 (64,116)	40 (64, 69)
3	μ	(30, 84)	470 (30, 90)	364.028	55.832	1.898	468 (30, 84)	459 (31, 95)	456 (10, 24)
	$\mu \pm 0.2\sigma$	(30, 84)	341 (30, 90)	228.028	47.871	2.360	335 (30, 85)	328 (31, 98)	320 (30, 79)
	$\mu \pm 0.4\sigma$	(30, 84)	234 (30, 91)	126.387	31.130	3.457	221 (30, 96)	217 (30, 86)	215 (30, 81)
	$\mu \pm 0.5\sigma$	(30, 84)	185 (30, 91)	84.089	23.384	4.315	176 (30, 84)	167 (30, 96)	166 (30, 64)

Table 13. Parking lot TV-to-IR correlation.

Method	Threshold	Expected Peak	1st Highest Peak	Average Value of Corr. Surface	Standard Deviation of Corr. Surface	S/N Ratio	2nd Highest Peak	3rd Highest Peak	4th Highest Peak
1	TL=150 TH=150	(35, 67)	311 (35, 68)	88.282	77.368	2.879	303 (35, 40)	302 (36, 55)	302 (36, 45)
	TL=200 TH=200	(35, 67)	227 (35, 65)	45.376	51.289	3.541	219 (35, 50)	212 (35, 44)	211 (35, 70)
2(a)	SL=1.0 SH=1.0	(35, 67)	493 (35, 67)	342.148	30.079	5.015	460 (35, 72)	460 (36, 62)	442 (35, 57)
	SL=1.0 SH=1.4	(35, 67)	444 (35, 67)	350.623	24.487	3.813	443 (36, 42)	430 (36, 47)	427 (36, 36)
2(b)	SL=1.0 SH=1.4	(35, 67)	105 (35, 67)	59.935	10.830	4.161	94 (41,132)	94 (35, 86)	93 (35, 72)
3	μ	(25, 47)	486 (35, 64)	365.767	45.458	2.645	478 (35, 69)	469 (33, 10)	467 (27, 47)
	$\mu \pm 0.2\sigma$	(25, 47)	414 (35, 68)	283.628	47.252	2.759	406 (35, 63)	397 (35, 75)	343 (34, 91)
	$\mu \pm 0.4\sigma$	(25, 47)	333 (27, 47)	200.216	42.473	3.126	323 (35, 69)	317 (34, 90)	317 (28, 17)
	$\mu \pm 0.5\sigma$	(25, 47)	266 (27, 48)	144.891	37.208	3.255	250 (34, 85)	249 (27, 43)	247 (34, 91)

Table 14. Water tower TV-to-IR correlation.

Method	Threshold	Expected Peak	1st Highest Peak	Average Value of Corr. Surface	Standard Deviation of Corr. Surface	S/N Ratio	2nd Highest Peak	3rd Highest Peak	4th Highest Peak
1	TL=150 TH=150	(43,124)	72 (43,108)	11.572	14.372	4.205	69 (1, 1)	68 (43,102)	68 (1, 14)
	TL=200 TH=200	(43,124)	43 (1, 74)	3.004	7.192	5.561	43 (1, 69)	43 (1, 64)	43 (1, 58)
2(a)	SL=1.0 SH=1.0	(43,124)	422 (51, 33)	339.898	16.721	4.910	400 (43,143)	398 (61, 38)	398 (28,112)
	SL=1.0 SH=1.4	(43,124)	394 (60, 1)	348.564	12.289	3.697	387 (60, 6)	387 (2,133)	387 (2, 3)
2(b)	SL=1.0 SH=1.4	(43,124)	362 (62, 4)	327.354	9.425	3.608	358 (59, 7)	356 (2,132)	355 (2, 13)
3	μ	(33,104)	421 (3, 56)	340.255	32.124	2.514	419 (3, 63)	416 (2, 90)	415 (43, 87)
	$\mu\pm0.2\sigma$	(33,104)	293 (5, 1)	227.734	27.791	2.348	292 (3, 58)	290 (33,103)	290 (4, 24)
	$\mu\pm0.4\sigma$	(33,104)	202 (33,104)	139.328	19.537	3.208	194 (3, 57)	187 (8, 2)	186 (7, 7)
	$\mu\pm0.5\sigma$	(33,104)	165 (33,104)	103.317	16.697	3.694	150 (3, 57)	144 (8, 2)	143 (42, 3)

Table 15. Rock quarry TV-to-IR correlation.

Method	Threshold	Expected Peak	1st Highest Peak	Average Value of Corr. Surface	Standard Deviation of Corr. Surface	S/N Ratio	2nd Highest Peak	3rd Highest Peak	4th Highest Peak
1	TL=150 TH=150	(49,117)	186 (30,122)	57.748	50.122	2.559	183 (31,133)	180 (31,128)	180 (30,138)
	TL=200 TH=200	(49,117)	90 (29,125)	19.114	20.520	3.454	87 (29,138)	83 (29,131)	83 (27,120)
2(a)	SL=1.0 SH=1.0	(49,117)	409 (2, 37)	339.586	18.027	3.836	403 (23, 29)	399 (2,129)	396 (7, 43)
	SL=1.0 SH=1.4	(40,117)	397 (23, 88)	347.241	14.917	3.334	397 (2, 37)	395 (23, 96)	394 (26, 76)
2(b)	SL=1.0 SH=1.4	(49,117)	77 (31, 78)	53.216	6.749	3.524	76 (6, 48)	75 (37, 49)	75 (30,116)
3	μ	(39, 87)	454 (39, 87)	342.917	32.933	3.373	445 (38, 92)	420 (37, 78)	419 (6, 32)
	$\mu \pm 0.2\sigma$	(39, 87)	331 (39, 87)	243.071	26.973	3.260	330 (37, 93)	308 (3, 38)	305 (5, 23)
	$\mu \pm 0.4\sigma$	(39, 87)	239 (37, 93)	166.106	22.167	3.288	237 (39, 87)	225 (3, 38)	218 (5, 32)
	$\mu \pm 0.5\sigma$	(39, 87)	189 (40, 84)	122.320	18.556	3.593	182 (39, 90)	176 (40, 96)	174 (37, 70)

IV. EFFECT OF QUANTIZATION TO SIXTEEN LEVELS

In this chapter, the effect on the performance of the correlator of quantizing videos to 16 levels is investigated. The digital images having pixels with quantized values ranging from 0 to 255 (256 levels, or 8 bits) were mapped to images having pixel values ranging from 0 to 15 (16 levels or 4 bits) using the three different methods. Mapped images were input to the correlation process and simulation results are presented in Tables 16 through 23.

Quantization by Truncation

The truncation method of mapping the original images quantized to 256 levels into images quantized to 16 levels is explained by Equation 19.

$$X(I,J) = k \quad \text{if } 16k \leq X(I,J) \leq 16k + 15 \qquad (19)$$

$$\text{for } k = 0, 1, 2, \ldots, 15$$

The NASA tower, parking lot, water tower and rock quarry scenes were transformed to 16 level images using Equation 19. Each scene was simulated using all three methods of thresholding previously discussed and the results are tabulated in Tables 16 through 19. Some important observations are listed below, method by method.

1. Method 1: (Threshold by intuition or trial-and-error)
Quantizing videos to 16 levels:

(a) did not have much effect on the correlation result for NASA tower scene and the performance is acceptable. Same is true for parking lot scene.

(b) did not lead to any meaningful results in the case of the water tank and rock quarry scenes. True peaks were not identified with original nor transformed images as inputs.

Method 2: (Threshold based on area average)

Quantizing videos to 16 levels:

(a) did have a negative effect on correlation process for NASA tower scene. When correlating using 256 level video, the true peak appeared for all considered values of SL and SH as one of the first four peaks. But when correlating using 16 level video, the true peak did not appear within the first four peaks of correlation surface for all values of SL and SH tried.

(b) did not have much effect on correlation results for parking lot scene and results are acceptable.

(c) again did not lead to any meaningful results in case of water tank and rock quarry scenes. True peaks were not identified in the original as well as transformed images as inputs.

Method 3: (Threshold based on means and standard deviations of gradient images)

Quantizing videos to 16 levels:

(a) improved the performance for NASA tower scene. For each value of S, the highest peak in the correlation surface was the true peak which is a definite improvement over previous results obtained by correlating 256 level images.

(b) did not have much effect on the correlation result for parking lot scene. Results were almost the same as before and the same is true for rock quarry scene.

(c) improved the performance for water tower scene with true peak appearing within the first four peaks for all values of S.

In general, quantizing videos to 16 levels by truncation did not deteriorate the performance. In fact, it improved the performance when correlating using the third method based on mean and standard deviation as a threshold to transform digital images to binary form.

Quantization Based on Dynamic Range of Pixel Range

As in the previous case the digital images having pixel values ranging from 0 to 255 (256 levels or 8 bits) were transformed to digital images of pixel values ranging from 0 to 15 (16 levels of 4 bits). Let L_1 be the pixel value such that approximately 1/16th of the total number of pixels in the original image have their values less than L_1 and let L_2 be the pixel value such that approximately 1/16th of the total number of pixels have their values greater than L_2. Then the range of pixel values from L_1 to L_2 represents the dynamic range of the original image. The quantization process is explained by Equation 20.

$$X(I,J) = \begin{cases} 0 & \text{if } X(I,J) < L_1 \\ k & \text{if } L_1 + \frac{L_2-L_1}{14}(k-1) \leq X(I,J) < L_1 + \frac{L_2-L_1}{14}k \\ & \text{for } k = 1, 2, \ldots, 14 \\ 15 & \text{if } X(I,J) \geq L_2 \end{cases} \qquad (20)$$

The four bit digital images obtained as explained by Equation 20, were used as inputs to the correlation process. Simulation results using the four scenes and the three methods considered in the previous sections are tabulated in Tables 20 through 23. Some salient observations are listed below for convenience, method by method.

1. Method 1: (Threshold by intuition or trial-and-error)

Quantizing videos to 16 levels:

(a) did not have much effect on final correlation results for NASA tower scene and the performance is acceptable.

(b) gave false peaks for parking lot scene. The true peak did not appear within the first four peaks in the correlation surface even after varying TL and TH from 8 to 20.

(c) improved the performance for water tower scene. True peak appeared as highest peak when TL and TH are equal to 15 and appeared as the third highest peak when TL and TH are equal to 20.

(d) did not lead to any meaningful results for the rock quarry scene. True peak was not identified with original nor the transformed images as inputs.

Comparison of four-bit vs. eight-bit quantization using this thresholding method is not conclusive since there may be a combination of values for TL and TH which were not tried in the simulations that would lead to better results.

2. Method 2: (Threshold based on area average)

Even though this method did not work as good as the third method, it is better than the first method. It is reasonable to compare the results obtained with 256 level video with that of 16 level video because this method is based on local average of 3 x 3 mask, not on guess work.

Quantizing videos to 16 levels:

(a) did have a negative effect on correlation process for the NASA tower scene. The true peak was within first four peaks for all cases

when correlated using 256 level video. However, when 16 level video was used as inputs, the true peak appeared as the highest peak only when SL and SH were equal to 1.0 and did not yield meaningful results for other values of SL and SH.

(b) did have a negative effect on correlation process for parking lot scene. It led to false peaks in two cases and true peak appeared as the third highest peak only when SL and SH equals 1.0. But when correlating using original 256 level video as inputs, true peak was the highest peak in all cases.

(c) did not lead us to any useful result in case of water tank and rock quarry scenes. True peaks went unidentified with original and transformed images as inputs.

In general, it can be stated that quantizing the video to 16 levels did have a negative effect on the correlation process.

3. Method 3: (Threshold based on mean and standard deviation of gradient images)

This is the best of the three methods discussed and gave satisfactory results for all scenes considered. The comparison of results obtained with original images as inputs to the correlation process with those obtained with 16 level images as inputs is reasonably fair and accurate. Quantizing video to 16 levels:

(a) had a slightly negative effect on correlation process for NASA tower scene. When correlated using 256 level video as inputs, the true peak was within the first four peaks for all four values of S. But when correlated using 16 level images as inputs, the true peak did

not appear within the first four peaks, when S equals 0.4 and 0.5.

(b) did not have much effect on the final correlation results for the parking lot scene and results are acceptable with the same being true for the water tower scene.

(c) did have a negative effect on the final results of rock quarry scene. When correlated using 256 level images, the true peak appeared as the highest peak for each of the cases with S equal to 0, 0.2 and 0.5. It appeared as the second highest peak for S equals 0.4. But this was not true when correlated using 16 level images as inputs.

It is extremely difficult to generalize anything based on just four scenes. With the scenes considered and simulation results obtained, it appears that quantization by truncation is better than this method.

Histogram Equalization

Using this method, the 256 levels of original image were mapped to 16 levels such that each level had approximately an equal member of pixels over a complete field of video. Since none of the thresholding methods yielded meaningful results for any of the four scenes, the simulation results are not included. For this method it was noticed that the means of the gradient arrays increased considerably. This may be due to one of the following reasons.

1. Edge points are enhanced to have a higher gradient value.
2. Artificial edges are introduced due to quantization error (i.e., quantization noise increased).

If the first reason were true, quantization to 4 bits would have lead to better results. Therefore it is concluded that the increased quantization error caused the poorer results.

Table 16. NASA tower TV-to-IR correlation with quantization to four bits by truncation.

Method	Threshold	Expected Peak	1st Highest Peak	Average Value of Corr. Surface	Standard Deviation of Corr. Surface	S/N Ratio	2nd Highest Peak	3rd Highest Peak	4th Highest Peak
1	TL=10 TH=10	(40,104)	125 (39,106)	19.761	26.931	3.908	119 (38, 81)	114 (39, 76)	112 (39,111)
	TL=12 TH=12	(40,104)	91 (38,106)	11.752	18.101	4.378	88 (41, 83)	86 (41, 94)	85 (41, 89)
2(a)	SL=1.0 SH=1.0	(40,104)	436 (21, 90)	368.301	15.705	4.311	430 (35,107)	421 (2,113)	420 (45, 67)
	SL=1.0 SH=1.4	(40,104)	447 (2, 93)	384.735	14.225	4.377	437 (34, 6)	436 (2,112)	435 (44, 90)
2(b)	SL=1.0 SH=1.4	(40,104)	76 (64, 60)	45.294	6.136	5.005	74 (64,120)	73 (64, 71)	72 (64,100)
3	μ	(30, 84)	511 (30, 84)	385.992	53.472	2.338	499 (30, 90)	485 (30, 79)	477 (31, 95)
	μ±0.2σ	(30, 84)	295 (30, 84)	190.364	36.354	2.878	293 (30, 90)	281 (30, 79)	279 (30, 95)
	μ±0.4σ	(30, 84)	295 (30, 84)	190.364	36.354	2.878	293 (30, 90)	281 (30, 79)	279 (30, 95)
	μ±0.5σ	(30, 84)	255 (30, 87)	146.949	24.816	4.354	238 (29, 79)	236 (30, 92)	235 (30, 65)

Table 17. Parking lot TV-to-IR correlation with quantization to four bits by truncation.

Method	Threshold	Expected Peak	1st Highest Peak	Average Value of Corr. Surface	Standard Deviation of Corr. Surface	S/N Ratio	2nd Highest Peak	3rd Highest Peak	4th Highest Peak
1	TL=10 TH=10	(35, 67)	321 (35, 67)	99.164	78.499	2.826	314 (35, 72)	313 (36, 55)	311 (36, 51)
	TL=12 TH=12	(35, 67)	270 (35, 65)	64.179	62.197	3.309	262 (35, 70)	257 (35, 51)	254 (35, 60)
2(a)	SL=1.0 SH=1.0	(35, 67)	496 (35, 67)	350.6	29.032	5.008	469 (35, 72)	466 (35, 62)	446 (35, 77)
	SL=1.0 SH=1.4	(35, 67)	454 (35, 66)	362.311	23.384	3.921	441 (36, 40)	437 (28, 30)	436 (35, 72)
2(b)	SL=1.0 SH=1.4	(35, 67)	102 (35, 68)	57.715	10.632	4.169	95 (35, 84)	93 (35, 63)	91 (35, 74)
3	μ	(25, 47)	480 (27, 48)	364.470	41.986	2.752	477 (35, 66)	468 (35, 61)	462 (35, 71)
	$\mu \pm 0.2\sigma$	(25, 47)	409 (35, 65)	277.060	40.672	3.244	399 (35, 70)	396 (35, 60)	393 (35, 84)
	$\mu \pm 0.4\sigma$	(25, 47)	256 (27, 45)	136.940	35.766	3.329	251 (27, 52)	249 (34, 89)	246 (34, 84)
	$\mu \pm 0.5\sigma$	(25, 47)	255 (27, 48)	114.608	32.608	3.385	216 (28, 42)	215 (27, 53)	210 (34, 90)

Table 18. Water tower TV-to-IR correlation with quantization to four bits by truncation.

Method	Threshold	Expected Peak	1st Highest Peak	Average Value of Corr. Surface	Standard Deviation of Corr. Surface	S/N Ratio	2nd Highest Peak	3rd Highest Peak	4th Highest Peak
1	TL=10 TH=10	(43,124)	87 (64, 36)	16.036	17.001	4.174	83 (64, 28)	81 (43,108)	79 (42,124)
	TL=12 TH=12	(43,124)	55 (1, 74)	6.396	10.032	4.845	55 (1, 68)	55 (1, 63)	55 (1, 57)
2(a)	SL=1.0 SH=1.0	(43,124)	415 (63, 19)	352.55	16.153	3.866	407 (54,107)	406 (33, 32)	405 (61, 47)
	SL=1.0 SH=1.4	(43,124)	416 (2, 44)	366.541	13.028	3.796	412 (63, 3)	412 (36, 73)	409 (55,128)
2(b)	SL=1.0 SH=1.4	(43,124)	74 (64, 38)	42.571	5.755	5.461	74 (64, 13)	73 (64, 49)	73 (64, 30)
3	μ	(33,104)	410 (33,102)	340.712	20.835	3.326	405 (43, 85)	404 (25, 11)	400 (18, 72)
	$\mu \pm 0.2\sigma$	(33,104)	248 (8, 1)	187.695	20.292	2.972	244 (1, 83)	238 (33,101)	237 (7, 7)
	$\mu \pm 0.4\sigma$	(33,104)	247 (33,104)	181.917	17.443	3.731	234 (43, 85)	234 (25, 16)	233 (34, 50)
	$\mu \pm 0.5\sigma$	(33,104)	214 (25, 13)	154.184	16.183	3.696	203 (2, 2)	199 (43, 84)	199 (33,104)

Table 19. Rock quarry TV-to-IR correlation with quantization to four bits by truncation.

Method	Threshold	Expected Peak	1st Highest Peak	Average Value of Corr. Surface	Standard Deviation of Corr. Surface	S/N Ratio	2nd Highest Peak	3rd Highest Peak	4th Highest Peak
1	TL=12 TH=12	(49,117)	203 (31,125)	71.803	56.545	2.320	202 (31,133)	199 (31,145)	198 (31,139)
	TL=10 TH=10	(49,117)	340 (31,131)	147.530	84.925	2.266	337 (31,137)	336 (31,145)	334 (30,122)
2(a)	SL=1.0 SH=1.0	(49,117)	414 (17, 87)	340.613	16.747	4.382	408 (27,139)	408 (32, 60)	394 (64, 99)
	SL=1.0 SH=1.4	(49,117)	406 (42, 24)	352.753	14.270	3.731	404 (17,65)	402 (50, 1)	402 (2,138)
2(b)	SL=1.0 SH=1.4	(49,117)	85 (64,131)	54.639	6.840	4.430	84 (64, 98)	83 (64,106)	81 (64, 55)
3	μ	(39, 87)	420 (39, 87)	336.392	28.397	2.944	411 (37, 94)	410 (43, 75)	406 (6, 39)
	μ±0.2σ	(39, 87)	299 (39, 87)	216.204	24.932	3.321	294 (37, 94)	274 (7, 52)	273 (1, 36)
	μ±0.4σ	(39, 87)	207 (40, 85)	141.240	18.905	3.478	204 (37, 93)	202 (36, 52)	188 (37, 72)
	μ±0.5σ	(39, 87)	161 (40, 85)	102.974	16.473	3.522	161 (37, 93)	150 (36, 54)	150 (21, 69)

Table 20. NASA tower TV-to-IR correlation with quantization to four bits over dynamic range.

Method	Threshold	Expected Peak	1st Highest Peak	Average Value of Corr. Surface	Standard Deviation of Corr. Surface	S/N Ratio	2nd Highest Peak	3rd Highest Peak	4th Highest Peak
1	TL=15 TH=15	(40,104)	120 (38,107)	17.583	24.715	4.144	112 (38,102)	105 (38, 80)	102 (38, 75)
	TL=20 TH=20	(40,104)	71 (42, 82)	8.358	13.205	4.744	69 (38,106)	65 (41, 88)	65 (38, 77)
2(a)	SL=1.0 SH=1.0	(40,104)	426 (39,106)	355.181	16.474	4.299	425 (38,122)	417 (39, 76)	415 (36, 91)
	SL=1.0 SH=1.4	(40,104)	595 (51, 76)	544.873	19.294	2.598	593 (55, 56)	592 (40,144)	590 (58,138)
2(b)	SL=1.0 SH=1.4	(40,104)	61 (64, 5)	31.262	5.475	5.432	60 (64, 34)	59 (64,113)	58 (64,104)
	μ	(30, 84)	513 (30, 91)	365.944	52.634	2.794	510 (30, 83)	510 (29, 65)	492 (30, 96)
	$\mu\pm0.2\sigma$	(30, 84)	413 (29, 63)	250.754	45.857	3.538	407 (30, 90)	406 (30, 84)	403 (29, 68)
	$\mu\pm0.4\sigma$	(30, 84)	260 (30, 52)	112.418	34.135	4.323	255 (30, 59)	249 (29, 65)	239 (30, 47)
	$\mu\pm0.5\sigma$	(30, 84)	26 (30, 52)	112.418	34.135	4.232	255 (30, 59)	249 (29, 65)	239 (30, 47)

Table 21. Parking lot TV-to-IR correlation with quantization to four bits over dynamic range.

Method	Threshold	Expected Peak	1st Highest Peak	Average Value of Corr. Surface	Standard Deviation of Corr. Surface	S/N Ratio	2nd Highest Peak	3rd Highest Peak	4th Highest Peak
1	TL=15 TH=15	(35, 67)	237 (8, 42)	92.321	51.816	2.792	228 (8, 47)	212 (8, 37)	212 (7, 52)
	TL=20 TH=20	(35, 67)	161 (41,145)	52.830	37.834	2.859	157 (41,140)	153 (8, 44)	151 (37,134)
2(a)	SL=1.0 SH=1.0	(35, 67)	470 (35, 76)	347.573	29.604	4.135	459 (35, 70)	456 (35, 14)	455 (42,124)
	SL=1.0 SH=1.4	(35, 67)	464 (39, 80)	362.017	25.353	4.023	456 (39,60)	453 (39, 74)	449 (39, 69)
2(b)	SL=1.0 SH=1.4	(35, 67)	99 (64, 64)	56.175	11.058	3.873	92 (14, 79)	91 (64, 74)	89 (14,103)
3	μ	(25, 47)	466 (34, 97)	356.371	36.572	2.998	465 (35, 68)	465 (34,105)	463 (33, 10)
	$\mu \pm 0.2\sigma$	(25, 47)	379 (27, 47)	261.961	35.624	3.285	375 (34,107)	373 (34, 98)	373 (34, 84)
	$\mu \pm 0.4\sigma$	(25, 47)	282 (22, 92)	172.488	32.397	3.380	281 (22, 87)	280 (27, 47)	274 (22, 97)
	$\mu \pm 0.5\sigma$	(25, 47)	259 (22, 92)	153.058	31.065	3.410	256 (27, 48)	255 (22, 87)	254 (22, 97)

Table 22. Water tower TV-to-IR correlation with quantization to four bits over dynamic range.

Method	Threshold	Expected Peak	1st Highest Peak	Average Value of Corr. Surface	Standard Deviation of Corr. Surface	S/N Ratio	2nd Highest Peak	3rd Highest Peak	4th Highest Peak
1	TL=15 TH=15	(43,124)	108 (42,124)	29.341	23.479	3.350	106 (64, 47)	106 (42,129)	100 (64, 42)
	TL=20 TH=20	(43,124)	54 (43,107)	8.043	9.324	4.924	54 (43,102)	50 (41,123)	47 (64, 48)
2(a)	SL=1.0 SH=1.0	(43,124)	407 (41, 37)	341.255	16.047	4.097	399 (51, 36)	397 (38, 79)	397 (1, 62)
	SL=1.0 SH=1.4	(43,124)	408 (39, 53)	354.118	12.736	4.231	401 (35,105)	398 (47,129)	398 (36,114)
2(b)	SL=1.0 SH=1.4	(43,124)	46 (64, 66)	29.006	4.522	3.758	46 (63,136)	44 (41, 78)	43 (58, 39)
3	μ	(33,104)	429 (3, 83)	347.918	32.233	2.515	429 (2, 78)	426 (4, 58)	424 (2, 28)
	$\mu \pm 0.2\sigma$	(33,104)	303 (3, 57)	219.568	25.608	3.258	287 (33,102)	279 (5, 27)	279 (3, 63)
	$\mu \pm 0.4\sigma$	(33,104)	266 (33,102)	193.004	20.433	3.572	266 (3, 57)	255 (41, 38)	253 (38, 48)
	$\mu \pm 0.5\sigma$	(33,104)	251 (3, 57)	169.956	22.718	3.567	230 (33,102)	227 (1, 73)	224 (3, 78)

Table 23. Rock quarry TV-to-IR correlation with quantization to four bits over dynamic range.

Method	Threshold	Expected Peak	1st Highest Peak	Average Value of Corr. Surface	Standard Deviation of Corr. Surface	S/N Ratio	2nd Highest Peak	3rd Highest Peak	4th Highest Peak
1	TL=12 TH=12	(49,117)	434 (30,141)	283.972	46.873	3.201	427 (30,136)	420 (30,125)	412 (29,130)
	TL=15 TH=15	(49,117)	272 (30,140)	137.188	43.734	3.083	265 (30,133)	263 (30,145)	256 (30,126)
2(a)	SL=1.0 SH=1.0	(49,117)	419 (2, 37)	340.974	18.509	4.216	410 (2,129)	403 (42, 59)	402 (45, 41)
	SL=1.0 SH=1.4	(49,117)	406 (34, 32)	351.039	15.484	3.550	404 (2,128)	400 (63, 7)	398 (34, 10)
2(b)	SL=1.0 SH=1.4	(49,117)	93 (64,120)	63.292	7.476	4.107	93 (64, 99)	91 (63, 63)	91 (63, 7)
3	μ	(37, 87)	426 (37, 93)	344.4	28.539	2.859	419 (7, 51)	411 (44, 3)	410 (37, 87)
	μ±0.2σ	(37, 87)	349 (37, 93)	257.316	24.798	3.697	328 (40, 85)	325 (38, 67)	322 (34, 76)
	μ±0.4σ	(37, 87)	275 (37, 93)	183.294	21.356	4.294	259 (40, 85)	252 (37, 66)	244 (23, 2)
	μ±0.5σ	(37, 87)	238 (37, 93)	150.708	20.216	4.318	226 (40, 85)	221 (37, 66)	217 (35, 72)

V. IMPROVED METHOD FOR TV-TO-IR CORRELATION

In TV-to-IR correlation alrogithms discussed in Chapter 3, the following three methods of choosing the gradient threshold used to transform gradient images to binary images were presented.

1. Threshold by intuition (trial-and-error)
2. Threshold based on average pixel value of nine pixels centered about the pixel of interest
3. Threshold based on mean and standard deviation of gradient array.

The performance of method three was better than that of the first two methods. However, the performance was not completely satisfactory. Even though the true peak appeared within the first four peaks of the correlation surface in all cases (256 level digital images), often the true peak did not appear as the highest peak. Also, the difference between the successive peaks is small. A method to bring out the true peak and to increase the difference in correlation value between successive peaks is discussed below and will be referred to as the improved method. This method is parallel to the one used in TV-to-TV correlation.

The correlation algorithm using a threshold based on mean and standard deviation of the gradient array was discussed in detail in Chapter 3. Some important points are rewritten in this section for convenience.

1(a) Mean and standard deviation are computed for the reference array of size K x L from GHRV.

(b) Thresholds THL and THH for GHRV are computed using Equations 21 and 22.

$$THL = \mu_H - S\,\sigma_H \tag{21}$$

$$THH = \mu_H + S\,\sigma_H \tag{22}$$

where, μ_H and σ_H are the mean and standard deviation of the reference.

S is a scaling factor ≥ 0 .

(c) The reference is quantized to two levels.

$$REFV\ (I,J) = \begin{cases} 1 & \text{if } REFV\ (I,J) \geq THH \\ 0 & \text{if } REFV\ (I,J) \leq THL \\ D & \end{cases}$$

where D's are don't cares.

2. The quantization procedure for GLRV is the same as that of REFV (or GHRV).

3. While correlating REFV with GLRV, only pixels with value zero or one are correlated with the corresponding pixel in GLRV. Don't cares are ignored because they represent uncertainty.

However, for better correlation results, the K x L reference from GHRV and each K x L sub-array from GLRV should be quantized in the same way to bring out similar image contents. That means, if the K x L reference is quantized based on its mean and standard deviation, each K x L sub-array of GLRV should be quantized based on its mean and standard deviation. This requires too much computation and cannot be

done in real-time with existing hardware. To reduce computation GLRV was quantized only once based on its mean and standard deviation. Simulation showed that the true peak did not always appear as the highest peak in the correlation surface, but it was within this first four peaks in all cases. A method to pull out the true peak from the four initial correlation peaks is explained below.

1. GHRV and GLRV are computed from reduced high resolution and low resolution video as explained in a previous chapter.

2. The mean and standard deviation of a K x L reference from GHRV are computed. THL and THH obtained from Equation 21 and 22 are used to quantize the reference.

3. Thresholds for GLRV, TLL and TLH are computed using the mean and standard deviation of the entire GLRV array. Then GLRV is quantized to zeros, ones and don't cares as before.

4. The binary images obtained in 2 and 3 are correlated using the algorithm described in Chapter 3.

5. A predetermined number of highest peaks and coordinates of their occurrence are identified from the cross correlation surface. In this simulation the first four peaks are used because the true peak appears as one of them in all cases. Let, (I_1,J_1), (I_2,J_2), (I_3,J_3) and (I_4,J_4) be the coordinates of the first four peaks.

6. Then a sub-array of size $(K+k) \times (L+\ell)$ beginning at $(I_1-k/2, J_1-\ell/2)$ is chosen. (In this simulation $k = \ell = 6$.) The mean and standard deviation of this sub-array are computed and used to obtain thresholds. The $(K+k) \times (L+\ell)$ sub-array is then quantized as before. A cross correlation

surface of size (k+1) x (ℓ+1) is computed by correlating the reference of size K x L with the sub-array of size (K+k) x (L+ℓ). The peak correlation value and its coordinates are identified. Let this be $R(I_1',J_1')$. $R(I_2',J_2')$, $R(I_3',J_3')$ and $R(I_4',J_4')$ are computed by repeating the above procedure using (K+k) x (L+ℓ) sub-arrays corresponding to (I_2,J_2), (I_3,J_3) and (I_4,J_4), respectively.

Simulation results to be presented next show that the improved method increases the probability of finding the true peak and reduces the probability of false peaks.

TV-to-IR Correlation Simulation Using Improved Method on 256 Level Video

Simulation results for the NASA tower, parking lot, water tower and rock quarry scenes before and after improved analysis with scale factor equal 0 and 0.2 are presented in Tables 24 and 25, respectively. In order to implement the improved method, gradient arrays have to be stored in memory. Even though it requires additional memory and computation, the following advantages make the improved method worthwhile.

1. Using the improved method on the four sub-arrays of GLRV corresponding to the four highest peaks obtained by initial correlation, yielded the true peak as the highest peak every time. Cases where the original correlation process yielded a false peak, but where the improved method yielded the correct peak are marked with an asterisk in Tables 24 through 25. In the Tables, the initial method is referred to as run 1 and the improved method as run 2.

2. In all but one out of 8 cases the first peak was higher using the improved method.

3. One measure of performance of a correlation technique is the ratio of the first peak to the second highest peak. Simulation shows that in all but one out of 8 cases this ratio is considerably higher after using the improved method.

4. The difference in correlation values between successive peaks increases which indicates better signal-to-noise ratio.

This can be better understood by referring to Figure 13, which is a plot of the first four peaks before and after improved analysis for the parking lot scene with a scale factor S equal to 0. The peak is expected at (25,47), but initial correlation yielded the highest peak at (35,64) with a correlation value of 486. True peak appeared as the fourth peak with a value of 467. However, the true peak appears as the highest peak with a value of 521 after using the improved method. The previous false peak at (34,64) now appears as third highest peak and its correlation value is 485.

Similar plots for all eight cases are shown in Figures 14 and 15. When the scale factor S is increased to 0.4 and 0.5, the improved method worked for a few cases and did not work for others. This is because the region of uncertainty, which is ignored while correlating, is small for sub-arrays chosen about the probable peaks as compared to that of the entire gradient array. Therefore, even if a higher scale factor is used to obtain initial peaks, a low scale factor should be used with the improved method.

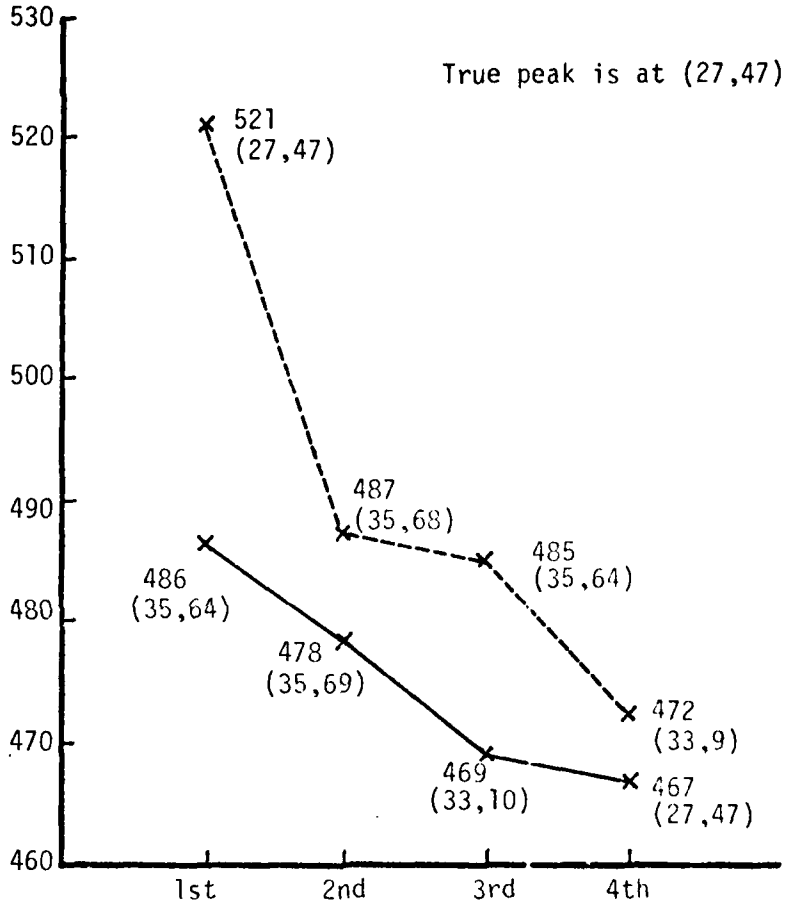

Figure 13. Plot of correlation values of first four peaks before and after improved analysis.

From the above simulations and analysis it is concluded that this improved method yields significantly better correlation results. It increases the probability of finding the true peak and reduces the probability of false peaks. It is recommended that MIRADCOM implement this procedure in their TV-to-IR correlator and test its performance on a large number of typical military scenes.

The improved correlation method consists of the following steps.

1. Perform an initial correlation on one or more fields by using the initial method of quantizing GLRV based on mean and standard deviation of the gradient array over one field. Store the last gradient array. Find N highest peaks by masking out a region about all previously determined peaks.

2. For the N highest peaks found in step one above (N can be any predetermined number and was four in the simulation) select N sub-gradient arrays of suitable size (greater than the size of reference). Requantize each of the sub-arrays using its mean and standard deviation to determine threshold. Pick the highest of each of N sub-correlation arrays.

3. Then find the largest of N correlation peaks and test for goodness of correlation.

This method yields a higher probability of finding the true peak and then reduces the probability of false peaks by limiting the dynamic search range.

TV-to-IR Correlation Using Improved Method for 16 Level Video

The effect of quantization to 16 levels was discussed in Chapter IV. It was concluded that, with the scenes considered and simulation results obtained, quantization by truncation was better than quantization using the complete dynamic range of the video. In this section improved analysis is made on 16 level video and results are presented. Tables 26 and 27 show the four peaks before and after improved analysis for the four 16 level scenes obtained by truncation using scale factors equal to 0 and 0.2, respectively. Some important observations are listed below.

1. Using the improved method on the four sub-arrays of GLRV corresponding to the four highest peaks yielded the true peak as highest peak in seven out of eight cases.
2. In all but one out of eight cases, the first peak was higher using the improved method.

The performance is acceptable. Plots of the four peaks before and after improved method are shown in Figures 16 and 17 for S equal 0 and 0.2, respectively. Slicing the dynamic range of pixel values to 16 levels had considerable negative effect on the performance of the correlator. Results before and after improved analysis are presented in Tables 28 and 29 and few important observations are listed below.

1. Using the improved method on the four sub-arrays of GLRV corresponding to the four initial peaks yielded the true peak as highest peak in only two out of eight cases.

2. In five out of eight cases, first peak was lower using the improved method.

Plots of the first four peaks before and after the improved method with scale factor S equal 0 and 0.2 are shown in Figures 18 and 19, respectively.

As concluded before, quantization of video to 16 levels by slicing the dynamic range of pixel values introduces more quantization noise and has considerable negative effect on the performance of the correlator.

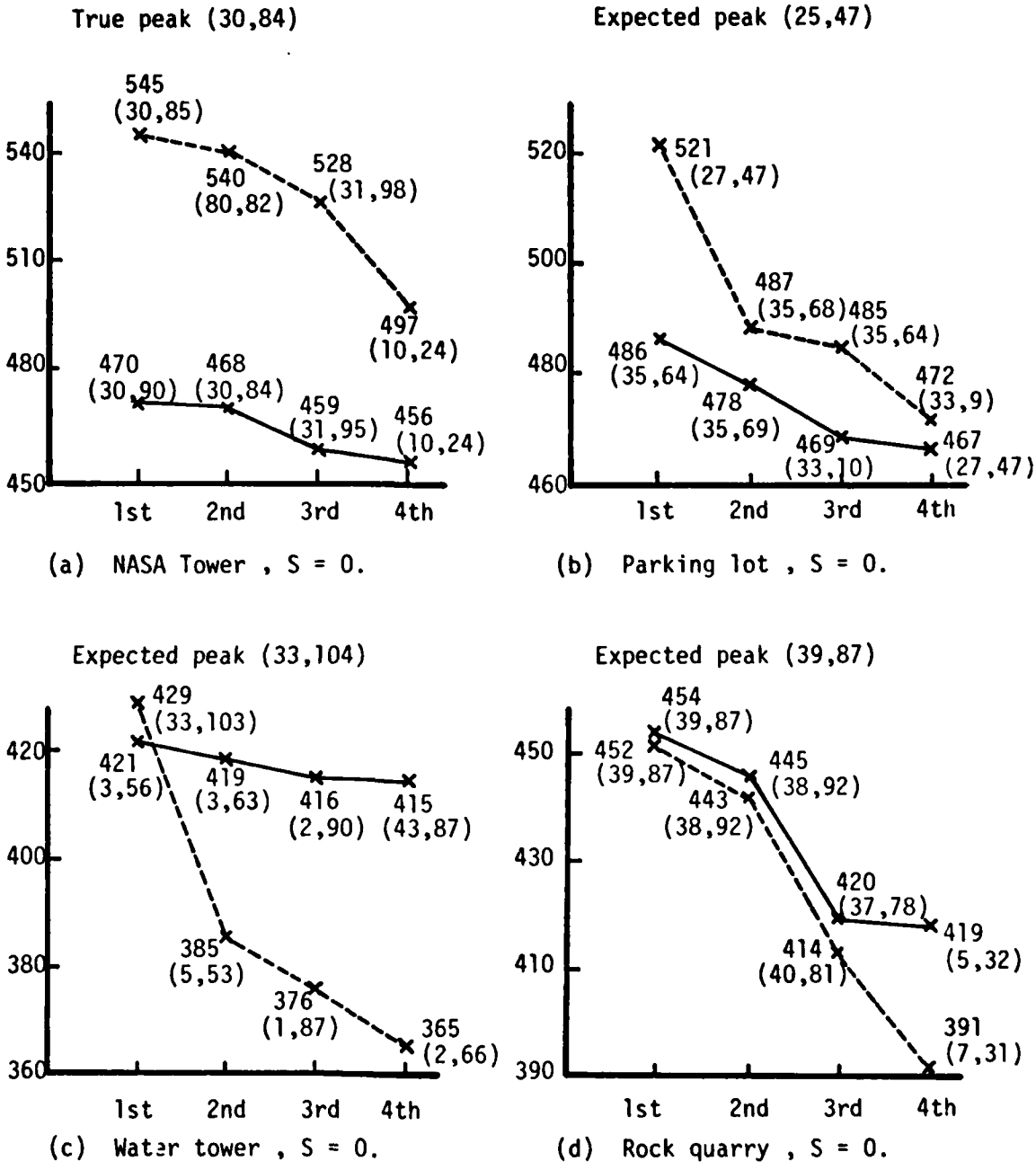

Figure 14. Correlation values of first four peaks before and after improved analysis.

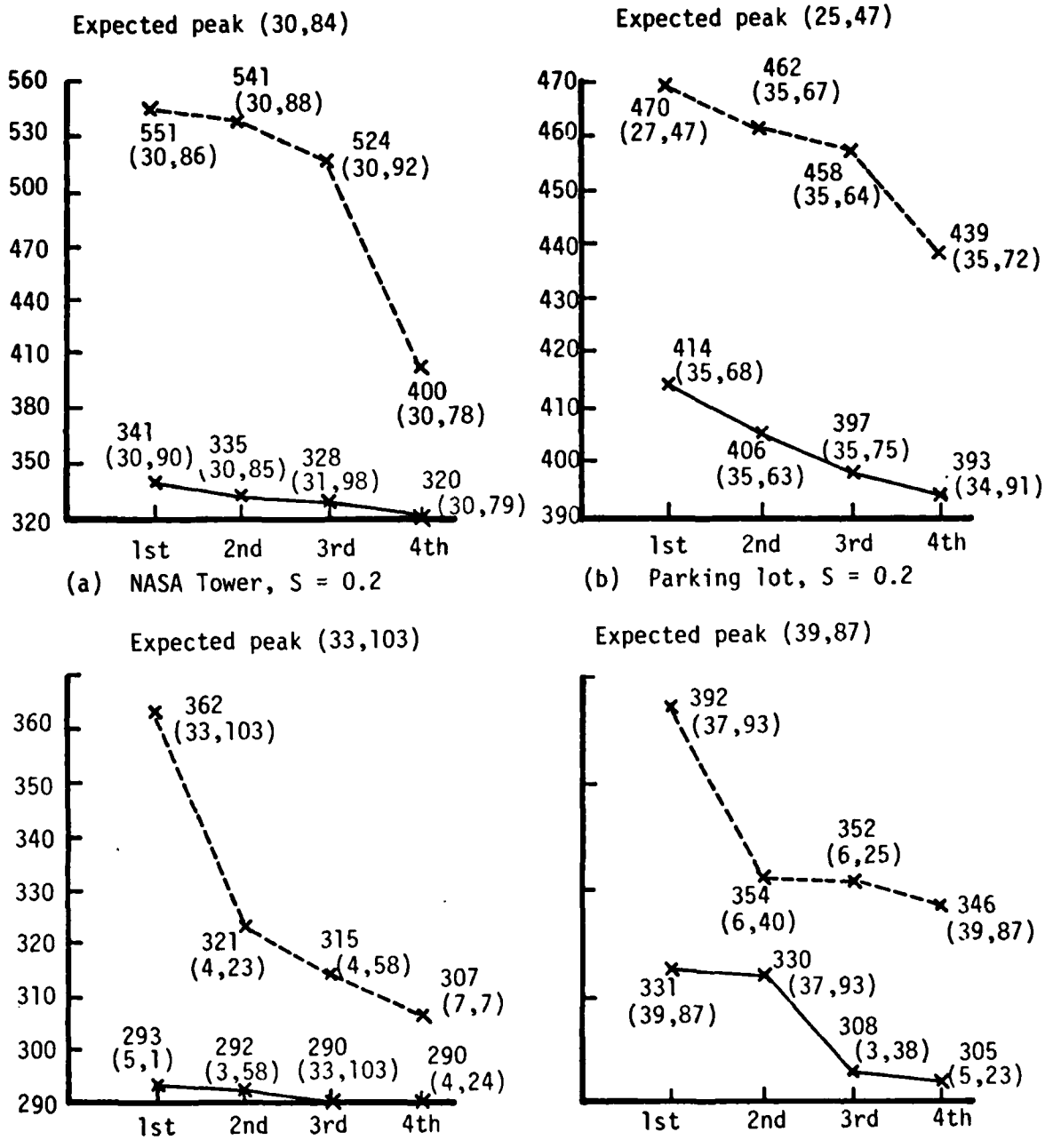

Figure 15. Correlation values of first four peaks before and after improved analysis.

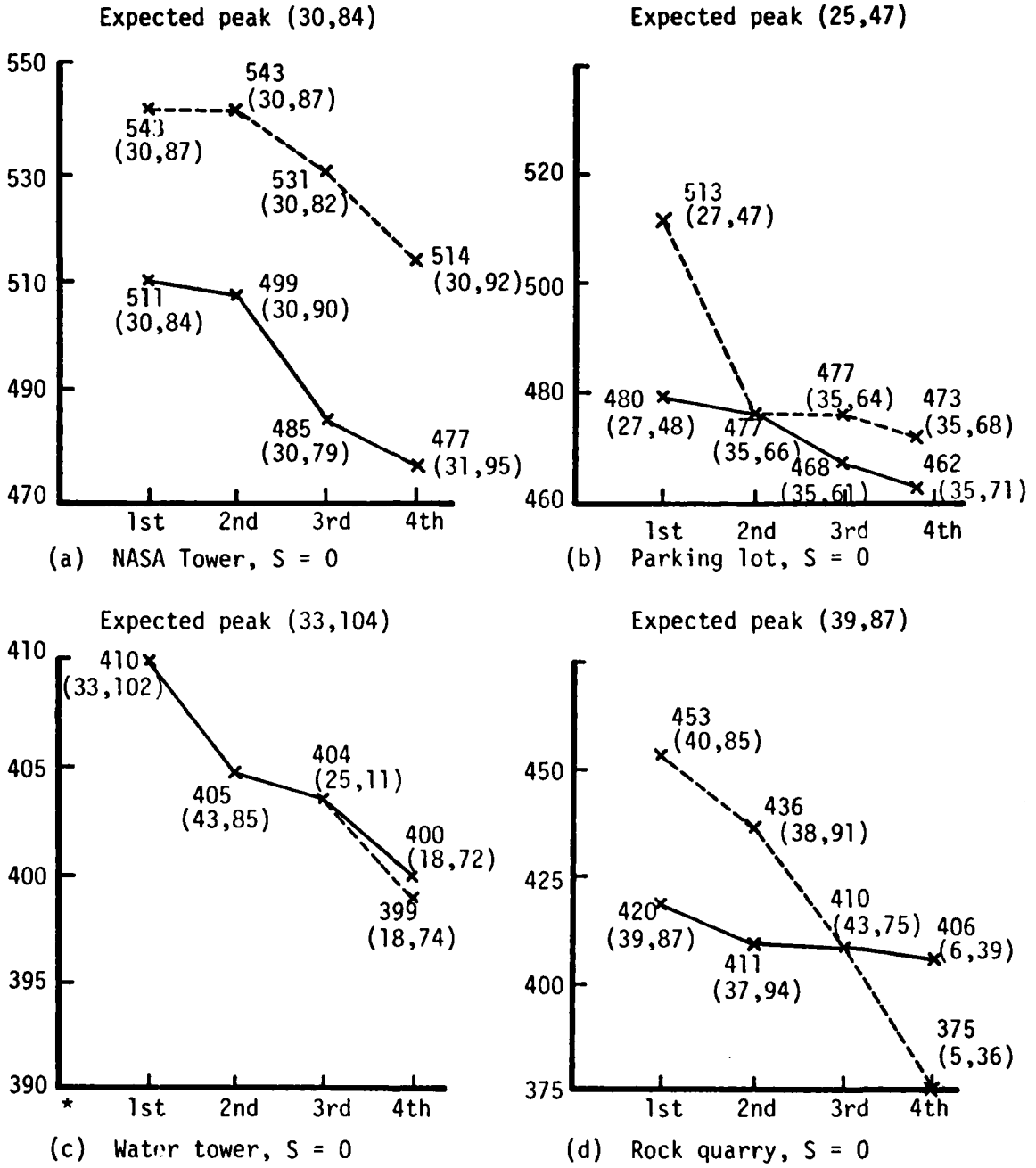

Figure 16. First four peaks before and after improved method for 16 level video (truncation).

* first 3 peaks overlap.

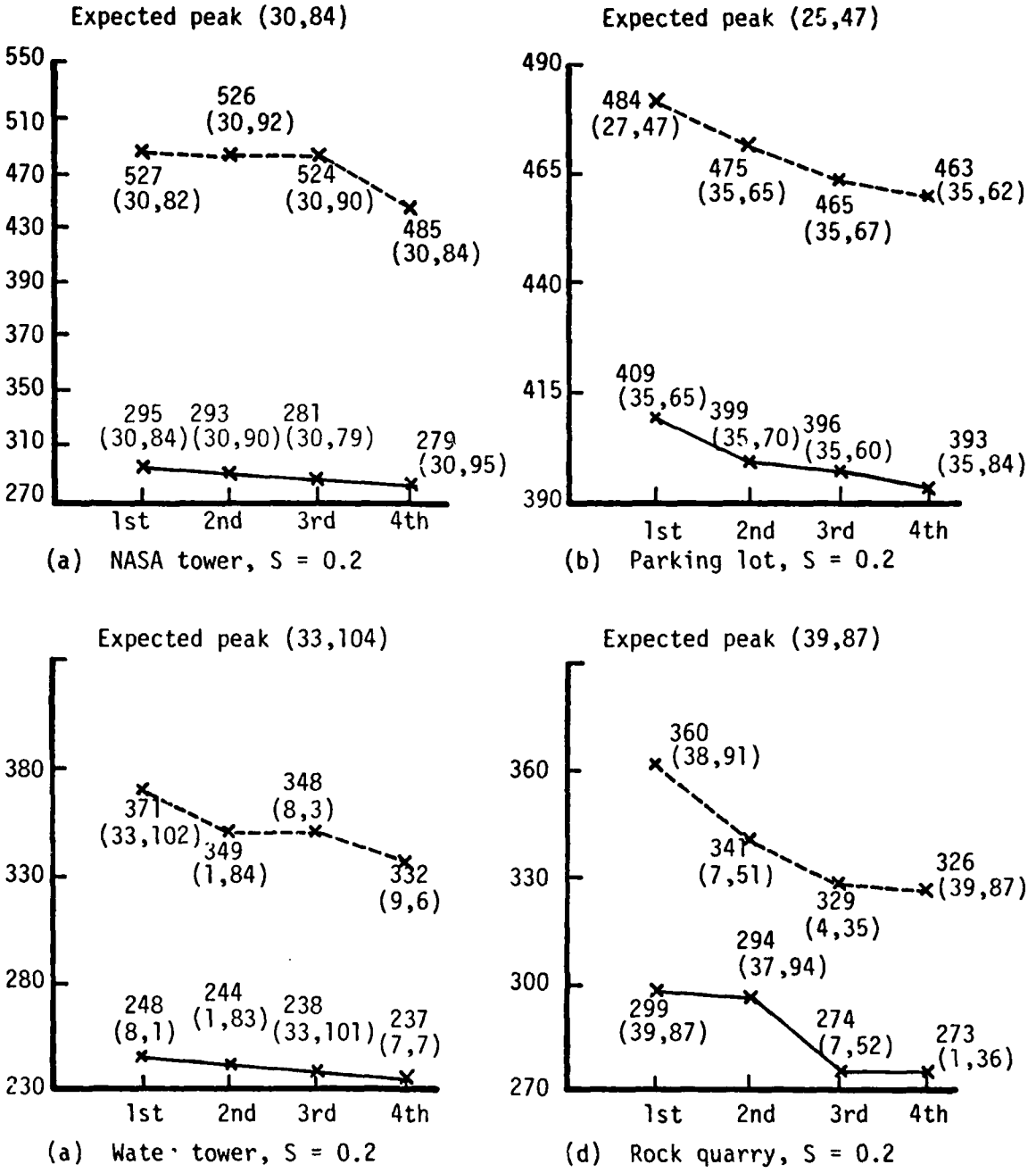

Figure 17. First four peaks before and after improved method for 16 level video (truncation).

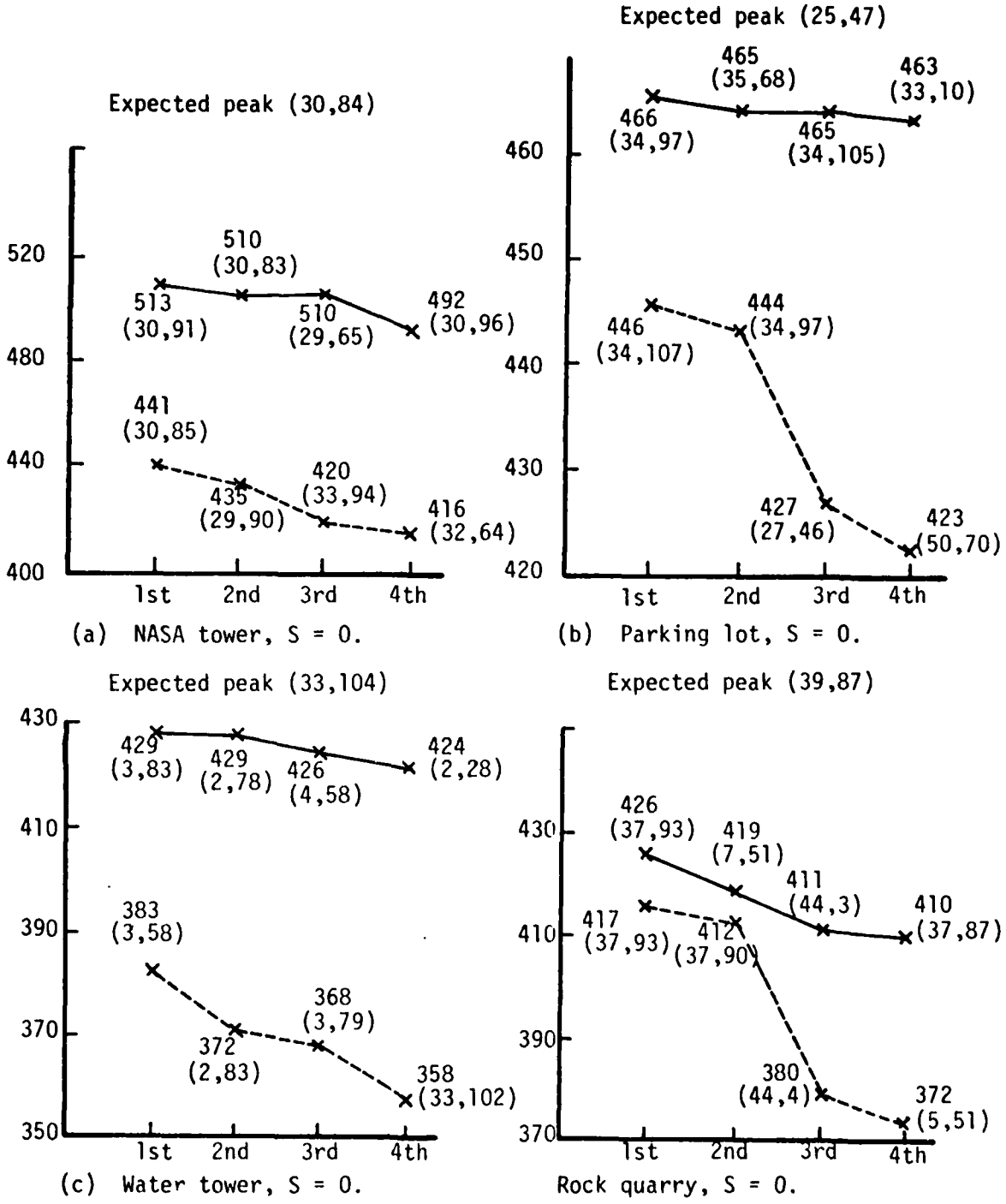

Figure 18. First four peaks before and after improved method for 16 level video (dynamic range slicing).

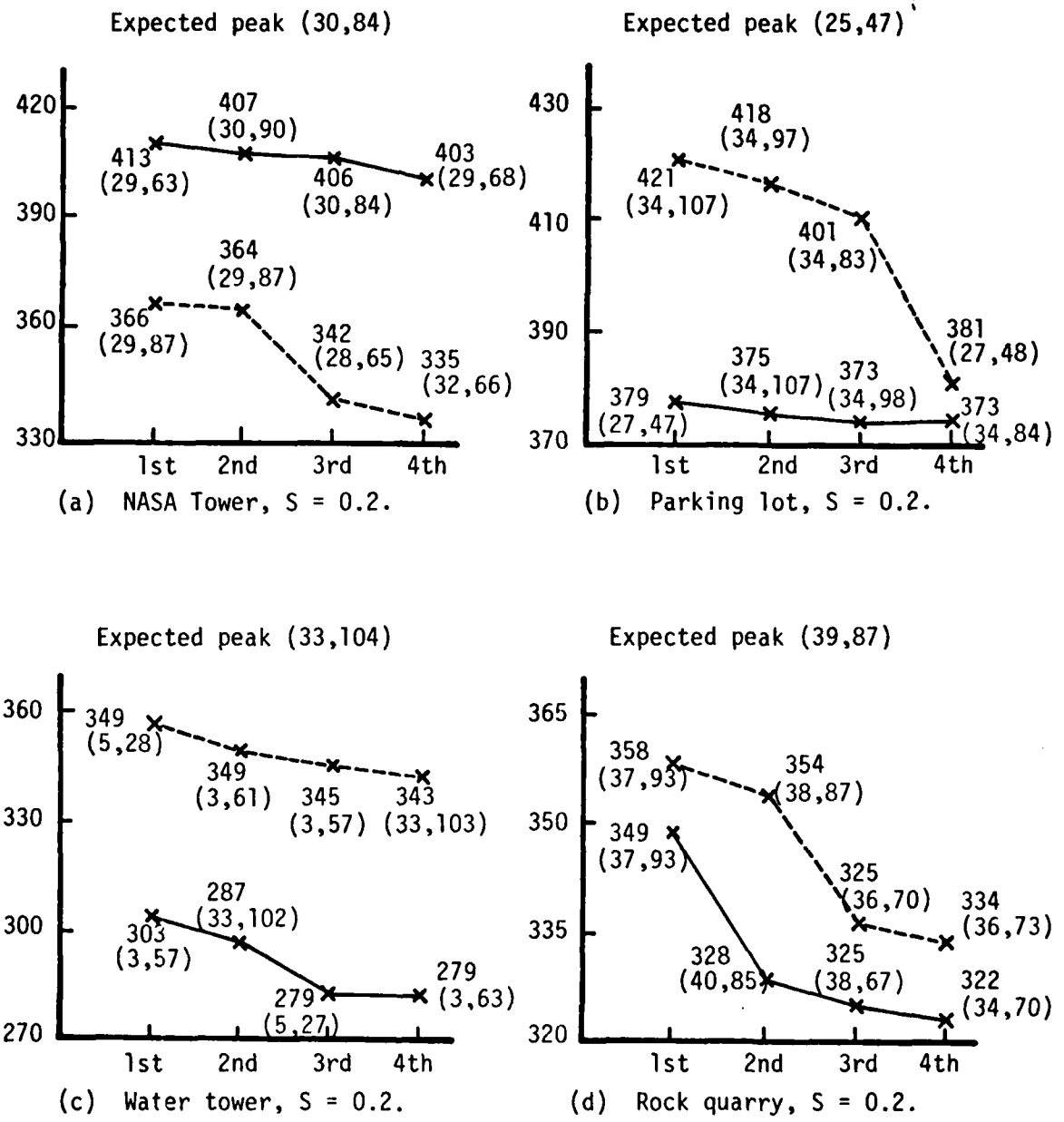

Figure 19. First four peaks before and after improved method for 16 level video (dynamic range slicing).

Table 24. TV-to-IR correlation using the improved method.

Scene	Run	True Peak	First Peak	Second Peak	Third Peak	Fourth Peak	Ratio of First Peak to Next Peak
NASA * tower	1	(30, 84)	470 (30,90)	468 (30,84)	459 (31,95)	456 (10,24)	1.0307
	2		545 (30,85)	540 (30,82)	528 (31,98)	497 (10,24)	1.0965
Parking * lot	1	(25, 47)	486 (35, 64)	478 (35,69)	469 (33,10)	467 (27,47)	1.0362
	2		521 (27, 47)	487 (35,68)	485 (35,64)	472 (33, 9)	1.0698
Water * tower	1	(33,104)	421 (3, 56)	419 (3,63)	416 (2,90)	415 (43,87)	1.0120
	2		429 (33,103)	385 (5,53)	376 (1,87)	365 (2,66)	1.114
Rock quarry	1	(39, 87)	454 (39, 87)	445 (38,92)	420 (37,78)	419 (6,32)	1.0835
	2		452 (39, 87)	443 (38,92)	414 (40,81)	391 (7,31)	1.1560

Table 25. TV-to-IR correlation using the improved method.

Scene	Run	True Peak	First Peak	Second Peak	Third Peak	Fourth Peak	Ratio of First Peak to Next Peak
NASA * tower	1	(30, 84)	341 (30, 90)	335 (30,85)	328 (31, 98)	320 (30,79)	1.0656
	2		551 (30, 86)	541 (30,88)	524 (30, 92)	400 (30,78)	1.3775
Parking * lot	1	(25, 47)	414 (35, 68)	406 (35,63)	397 (35, 75)	393 (34,91)	1.0534
	2		470 (27, 47)	462 (35,67)	458 (35, 64)	439 (35,72)	1.0173
Water * tower	1	(33,104)	293 (5, 1)	292 (3,58)	290 (33,103)	290 (4,24)	1.0034
	2		362 (33,103)	321 (4,23)	315 (4, 58)	307 (7, 7)	1.1277
Rock quarry	1	(39, 87)	331 (39, 87)	330 (37,93)	308 (3, 38)	305 (4,23)	1.0747
	2		392 (37, 93)	354 (6,40)	352 (6, 25)	346 (39,87)	1.1073

Table 26. TV-to-IR correlation using the improved method for 16 level video obtained by truncation.

Scene	Run	True Peak	First Peak	Second Peak	Third Peak	Fourth Peak	Ratio of First Peak to Next Peak
NASA tower	1	(30, 84)	511 (30, 84)	499 (30,90)	485 (30,79)	477 (31, 95)	1.0713
	2		543 (30, 87)	543 (30,87)	531 (30,82)	514 (30, 92)	1.0564
Parking lot	1	(25, 47)	480 (27, 48)	477 (35,66)	468 (35,61)	462 (35, 71)	1.0063
	2		513 (27, 47)	477 (35,66)	477 (35,64)	473 (35, 68)	1.0755
Water tower	1	(33,104)	410 (33,102)	405 (43,85)	404 (25,11)	400 (18, 72)	1.0123
	2		410 (33,102)	405 (43,85)	404 (25,11)	399 (18, 74)	1.0123
Rock quarry	1	(39, 87)	420 (39, 87)	411 (37,94)	410 (43,75)	406 (6, 39)	1.0219
	2		453 (40, 85)	436 (38,91)	410 (43,75)	375 (5, 36)	1.1048

Table 27. TV-to-IR correlation using improved method for 16 level video obtained by truncation.

Scene	Run	True Peak	First Peak	Second Peak	Third Peak	Fourth Peak	Ratio of First Peak to Next Peak
NASA tower	1	(30, 84)	295 (30, 84)	293 (30,90)	281 (30, 79)	279 (30,95)	1.0573
	2		527 (30, 82)	526 (30,92)	524 (30, 90)	485 (30,84)	1.0019
Parking * lot	1	(25, 47)	409 (35, 65)	399 (35,70)	396 (35, 60)	393 (35,84)	1.0407
	2		484 (27, 47)	475 (35,65)	465 (35, 67)	463 (35,62)	1.0189
Water * tower	1	(33,104)	248 (8, 1)	244 (1,83)	238 (33,101)	237 (7, 7)	1.0164
	2		371 (33,102)	349 (1,84)	348 (8, 3)	332 (9, 6)	1.0630
Rock quarry	1	(39, 87)	299 (39, 87)	294 (37,94)	274 (7, 52)	273 (1,36)	1.0912
	2		360 (38, 91)	341 (7,51)	329 (4, 35)	326 (39,87)	1.0557

Table 28. TV-to-IR correlation using improved method for 16 level video obtained by slicing the dynamic range.

Scene	Run	True Peak	First Peak	Second Peak	Third Peak	Fourth Peak	Ratio of First Peak to Next Peak
NASA * tower	1	(30, 84)	513 (30, 91)	510 (30,83)	510 (29, 65)	492 (30, 96)	1.0059
	2		441 (30, 85)	435 (29,90)	420 (33, 94)	416 (32, 64)	1.0138
Parking lot	1	(25, 47)	466 (34, 97)	465 (35,68)	465 (34,105)	463 (33, 10)	1.0021
	2		446 (34,107)	444 (34,97)	427 (27, 46)	423 (35, 70)	1.0045
Water tower	1	(33,104)	429 (3, 83)	429 (2,78)	426 (4, 58)	424 (2, 28)	1.0070
	2		383 (3, 58)	372 (2,83)	368 (3, 79)	358 (33,102)	1.0296
Rock quarry	1	(39, 87)	426 (37, 93)	419 (7,51)	411 (44, 3)	410 (37, 87)	1.0167
	2		417 (37, 93)	412 (37,90)	380 (44, 4)	372 (5, 51)	1.0973

Table 29. TV-to-IR correlation using the improved method for 16 level video obtained by slicing the dynamic range.

Scene	Run	True Peak	First Peak	Second Peak	Third Peak	Fourth Peak	Ratio of First Peak to Next Peak
NASA * tower	1	(30, 84)	413 (29, 63)	407 (30, 90)	406 (30,84)	403 (29, 68)	1.0147
	2		366 (29, 87)	364 (29, 87)	342 (28,65)	335 (32, 66)	1.0702
Parking lot	1	(25, 47)	379 (27, 47)	375 (34,107)	373 (34,98)	373 (34, 84)	1.0107
	2		421 (34,107)	418 (34, 97)	401 (34,83)	381 (27, 48)	1.0072
Water tower	1	(33,104)	303 (3, 57)	287 (33,102)	279 (5,27)	279 (3, 63)	1.0557
	2		356 (5, 28)	349 (3, 61)	345 (3,57)	343 (33,103)	1.0201
Rock quarry	1	(39, 87)	349 (37, 93)	328 (40, 85)	325 (38,67)	322 (34, 70)	1.0738
	2		358 (37, 93)	354 (38, 87)	338 (36,70)	334 (36, 73)	1.0592

VI. CONCLUSIONS AND RECOMMENDATIONS

Most of the conclusions and recommendations resulting from the work on this contract have been given and justified within the first five chapters of this report.

1. In chapter 2, an improved method for TV-to-TV correlation is recommended. From simulation and analysis it is concluded that the improved method yields significantly better correlation results than previous methods by increasing the probability of finding the true peak and reducing the probability of false peaks.

2. Sensitivity of the correlator to field of view errors was investigated. Simulation results showed that the correlator is relatively insensitive to scale factor errors of up to $\pm$5%.

3. In Chapter 3, three algorithms for TV-to-IR correlation are developed. Method 3, where gradient arrays are quantized based on their mean and standard deviation, was found promising. Even though this method involves more computation, the problem of choosing gradient threshold became simpler than before.

4. In Chapter 5, an improved method similar to the one in TV-to-TV correlation is developed for TV-to-IR correlation. The improved method yielded significantly better correlation results. Probability of finding the true peak increased considerably.

5. The effect of quantizing the video to 16 levels on correlator performance is investigated in Chapter 4. Transformation of 256 levels

to 16 levels was accomplished in the following three ways:

a. Truncation

b. Dynamic range slicing

c. Histogram equalization to 16 levels.

The first method had little effect on the performance of the correlator and was acceptable. After improved analysis true peak was identified as highest peak. Method 2 had considerable negative effect on the performance of correlator. Even the improved method did not yield satisfactory results. Quantization by histogram equalization was totally unsatisfactory. Therefore, it is concluded that the method of quantizing video to 16 levels is critical and should be given careful consideration before implementing in hardware.


DATE
FILME
8-8